ĐẠI HỌC HUẾ

VIỆN CÔNG NGHỆ SINH HỌC

NGUYỄN QUANG HOÀNG VŨ

DANH MỤC CÁC BÀI BÁO, CÔNG TRÌNH LIÊN QUAN ĐẾN LUẬN ÁN

Tên luận án: Nghiên cứu ảnh hưởng của vật liệu nano bạc đến một số bệnh hại trên cây sen (*Nelumbo nucifera*) trồng ở Thừa Thiên Huế

Chuyên ngành: Sinh học

Mã số: 9420101

Huế, 2025

DANH MỤC CÁC CÔNG TRÌNH/BÀI BÁO CÔNG BỐ LIÊN QUAN ĐẾN LUẬN ÁN

[1]. **Nguyễn Quang Hoàng Vũ**, Hoàng Tấn Quảng, Hoàng Thị Kim Hồng (2021). **Hiệu quả kháng nấm của vật liệu nano bạc lên nấm *Curvularia lunata* gây bệnh đốm lá phân lập trên giống sen trắng (*Nelumbo nucifera*) trồng tại Thừa Thiên Huế**. Báo cáo đăng toàn văn tại Hội nghị khoa học toàn quốc về Công nghệ sinh học, trang 861 – 867.

[2]. **Vu Nguyen Quang Hoang**, Quang Hoang Tan, Hong Hoang Thi Kim, Agarie Sakae (2022). **Microbiology associated with disease on white lotus (*Nelumbo nucifera* Gaertn.) and application of silver nanoparticles for controlling plant pathogens *in vitro***. Journal of the Faculty of Agriculture, Kyushu University, 67 (2), 165–172. https://doi.org/10.5109/4797823.

[3]. **Vu Quang Hoang Nguyen,** Tram Thi Ngoc Tran, Lan Thuy Tran, Thi Thi Diem Pham, Quang Tan Hoang, Hong Thi Kim Hoang (2023)**. *Neofusicoccum parvum*: a novel pathogen species causing wilted leaves and dieback petioles on lotus (*Nelumbo nucifera*) in Thua Thien Hue, Vietnam**. Hue University Journal of Science: Agriculture and Rural Development. Vol. 132, No. 3C, 2023, pp. 51–67, https://doi.org/10.26459/hueunijard.v132i3C.7275

[4]. **Vu Quang Hoang Nguyen**, Quang Tan Hoang, Lan Thuy Tran, Tram Tran Thi Ngoc, Hoang Thi Kim Hong (2024). **Molecular phylogeny of *Lasiodiplodia theobromae* associated with *Nelumbo nucifera* in Thua Thien Hue, Vietnam, and their sensitivity to silver nanoparticles**. Báo cáo toàn văn Hội nghị khoa học toàn quốc về Công nghệ sinh học, pp. 1135-1141

[5]. **Vu Quang Hoang Nguyen,** Thi Thi Diem Pham, Lan Thuy Tran, Tram Thi Ngoc Tran, Hoang Tan Quang, Hoang Thi Kim Hong (2025). **First report of *Colletotrichum plurivorum* causing anthracnose on the aquatic plant (*Nelumbo nucifera*) from Vietnam.** *Journal of Phytopathology* 173, No. 5: e70177. https://doi.org/10.1111/jph.70177.

HIỆU QUẢ CỦA VẬT LIỆU NANO BẠC LÊN NẤM *CURVULARIA LUNATA* GÂY BỆNH ĐỐM LÁ PHÂN LẬP TRÊN GIỐNG SEN TRẮNG (*NELUMBO NUCIFERA*) TRỒNG TẠI THỪA THIÊN HUẾ

Nguyễn Quang Hoàng Vũ[1], Hoàng Tấn Quảng[1], Hoàng Thị Kim Hồng[2]*

[1]Viện Công nghệ Sinh học, Đại học Huế

[2]Khoa Sinh học, Trường Đại học Khoa học, Đại học Huế

TÓM TẮT

Nghiên cứu này tiến hành nhằm xác định đối tượng gây bệnh đốm lá trên cây Sen Trắng trồng tại Thừa Thiên Huế và nghiên cứu hiệu quả kháng nấm trong điều kiện *in vitro* của vật liệu nano bạc. Quá trình thu thập mẫu, phân lập trên môi trường Potato Dextrose Agar (PDA) cho thấy tản nấm ban đầu có màu xám nhạt sau đó chuyển thành màu xanh đậm, khuẩn ty mọc thẳng, màu nâu sẫm, có hình vòng cung và không phân nhánh. Bào tử có dạng oliu, hình móc câu, vách nhẵn, màu nâu sẫm, 3 - 4 ngăn, có kích thước khoảng 20 - 25 µm × 8,5 - 12 µm. Định danh bằng kỹ thuật sinh học phân tử với cặp mồi ITS1-ITS4 cho thấy nấm gây hại là *Curvularia lunata*. Theo hiểu biết của chúng tôi, đây là báo cáo đầu tiên về nấm *Curvularia lunata* gây bệnh đốm lá trên cây Sen Trắng (*Nelumbo nucifera*) ở Việt Nam. Kết quả thử nghiệm đánh giá khả năng kháng nấm trong điều kiện *in vitro* bằng cách sử dụng vật liệu nano bạc được tiến hành khảo sát ở 5 nồng độ: 0,1 mg/L, 1 mg/L, 10 mg/L, 20 mg/L và 30 mg/L. Cả 5 nồng độ nano bạc đều cho thấy khả năng ức chế nấm bệnh, với hiệu lực ức chế tăng dần tương ứng với sự gia tăng nồng độ nano bạc. Xử lý nano bạc ở nồng độ 20 mg/L hiệu lực ức chế nấm *Curvularia lunata* lên đến 68,32% và 61,47% tương ứng ở thời điểm 3 ngày và 5 ngày theo dõi, nồng độ 30 mg/L hiệu lực ức chế lên đến 91,37% và 93,21%. Như vậy, vật liệu nano bạc thực sự có hiệu quả trong việc ức chế sự sinh trưởng của loài nấm *Curvularia lunata* gây bệnh đốm lá và có tiềm năng ứng dụng như một giải pháp xanh để kiểm soát bệnh hại thực vật.

Từ khóa: bệnh đốm lá, *Curvularia lunata*, kháng nấm, nano bạc, *Nelumbo nucifera*, Thừa Thiên Huế, sen trắng

MỞ ĐẦU

Cây sen (*Nelumbo nucifera*) là một loài thực vật thủy sinh đa niên, có hoa đẹp, thanh khiết, là biểu tượng gắn liền với Phật Giáo cũng như văn hóa và lịch sử. Bên cạnh giá trị làm cảnh, cây sen còn có nhiều giá trị kinh tế cao với sự đa dạng sản phẩm đặc sản địa phương và các yếu tố liên quan đến cảnh quan sinh thái. Đặc biệt, trong số các giống sen ở Thừa Thiên Huế thì giống Sen Trắng (chủ yếu là giống Sen Trắng Trẹt Lõm), một giống sen bản địa mang thương hiệu đặc trưng với hương thơm đặc trưng, hạt có mùi vị ngon, ngọt, bùi và dẻo [1]. Tuy nhiên, do sự cạnh tranh của các giống sen cao sản được du nhập từ các vùng miền khác vào trồng ở Huế, cũng như sự ô nhiễm của các sông hồ, ruộng trồng sen trắng trong những năm gần đây đã dần dần thu hẹp diện tích trồng. Thêm vào đó, quá trình sinh trưởng và sản lượng thu hoạch sen chịu ảnh hưởng lớn bởi tác động của sâu và nấm bệnh thực vật. Năm 2019, một số diện tích sen ở Thừa Thiên Huế có hiện tượng chết, bệnh với tỷ lệ lớn, có nhiều vùng tỷ lệ chết lên đến 50 - 70 %, trong đó diện tích sen chết tập trung nhiều nhất là ở các xã Phong Sơn, Phong Hiền với diện tích sen chết lần lượt là 51 ha, 40 ha. Để diệt nguồn sâu hại hay nấm, phương thức xử lý được áp dụng phổ biến hiện nay là sử dụng các loại thuốc diệt nấm, thuốc trừ sâu tổng hợp. Các phương thức giải quyết này thường dẫn đến các vấn đề về kháng thuốc và gia tăng chi phí xử lý môi trường do tàn dư lượng thuốc còn lại trong môi trường, ngoài ra còn tác động không mong muốn đến các đối tượng ngoài mục tiêu.

Trong khi đó các vật liệu nano nổi lên gần đây với nhiều báo cáo về những đặc tính kháng khuẩn, kháng nấm và sự hiệu quả trong quản lý bệnh hại, tiêu biểu là vật liệu nano bạc (AgNPs) với đặc tính kháng khuẩn đặc trưng và diện tích bề mặt lớn đã được minh chứng và tăng hiệu quả ở liều thấp, hứa hẹn sẽ cung cấp một giải pháp thay thế giúp kiểm soát bệnh hại thực vật, thân thiện với môi trường [2]. Từ những lý do trên, chúng tôi nghiên cứu tiến hành phân lập định loại mẫu bệnh, và đánh giá ảnh hưởng của vật liệu nano bạc với nấm *Curvularia lunata* gây bệnh đốm lá sen. Kết quả của nghiên cứu này là cơ sở khoa học cần thiết để có thể xây dựng biện pháp kiểm soát bệnh hại cây trồng khác nhau do nấm gây ra giúp khai thác tối đa tiềm năng kinh tế, văn hóa của giống Sen Trắng trồng ở Thừa Thiên Huế.

NGUYÊN LIỆU VÀ PHƯƠNG PHÁP

Vật liệu thí nghiệm:

Vật liệu nano bạc được cung cấp bởi bộ môn Vật lý chất rắn, Khoa Vật lý, Trường Đại học Khoa học, Đại học Huế, hạt nano có đường kính từ 4 - 5 nm. Vật liệu nano được tổng hợp từ bạc nitrat ($AgNO_3$) và tác nhân khử là dịch chiết từ lá cây nha đam (*Aloe barbadensis* Miller). Nồng độ dung dịch nano bạc gốc là 40 mg/L.

Mẫu bệnh sen được thu tại ruộng trồng Sen Trắng tại xã Phong Hiền, huyện Phong Điền, tỉnh Thừa Thiên Huế.

Địa điểm nghiên cứu:

Các thí nghiệm phân lập được tiến hành tại phòng thí nghiệm Công nghệ Enzyme - Protein. Quá trình tách chiết DNA, định danh phân tử được tiến hành tại phòng thí nghiệm Công nghệ Gen, Viện Công nghệ sinh học, Đại học Huế.

Phương pháp

Phương pháp điều tra, thu thập mẫu

Thu thập: Các mẫu sen có biểu hiện bệnh đốm lá (chọn các mẫu có vết bệnh mới) được thu thập tại các ruộng trồng sen tại xã Phong Hiền, huyện Phong Điền, tỉnh Thừa Thiên Huế. Mẫu bệnh thu nhận được đựng trong túi plastic, dán nhãn, chuyển về phòng thí nghiệm và bảo quản ở 4℃ để tiến hành phân lập. Các triệu chứng và biểu hiện bệnh cũng được ghi chép và ghi nhận bằng hình ảnh ngay tại điểm thu mẫu để so sánh, đối chiếu.

Thời gian điều tra: Điều tra định kỳ 7 ngày/lần ở tuyến điều tra trong khu vực điều tra.

Phương pháp phân lập nấm bệnh

Phương pháp phân lập được tiến hành theo Burgess và đồng tác giả (2008) [3]. Các mẫu bệnh thu thập được rửa sạch bằng nước, sau đó tiến hành khử trùng bề mặt mẫu qua các bước: ngâm trong hỗn hợp dung dịch natri hypochlorite 1% và ethanol 10% (1 - 5 phút), rồi rửa lại bằng nước cất vô trùng. Cắt nhỏ mô bệnh thành mảnh nhỏ kích thước 5 mm x 5 mm (chọn vùng ráp gianh giữa mô bệnh và mô khỏe). Đặt các mảnh mô vào môi trường thạch khoai tây PDA (200 g khoai tây, 20 g D- Glucose, 15 g Agar) và tiến hành ủ các đĩa ở nhiệt độ 27 ± 2℃ trong vòng 96 giờ để nấm bệnh phát triển. Khi nấm đạt đường kính tản nấm 1 - 2 cm, cấy truyền sang môi trường PDA mới. Làm thuần mẫu nấm bằng cách cấy đỉnh sinh trưởng của một sợi nấm từ môi trường cũ sang môi trường PDA mới.

Phương pháp định danh phân tử bằng kỹ thuật PCR:

Tách chiết DNA: Mẫu được nghiền trong CTAB buffer theo phương pháp của Doyle& Doyle (1987) [4].

Các mẫu nấm thuần phân lập được định danh bằng cách khuếch đại với cặp primer ITS1 và ITS4.

ITS1 (forward): 5'- TCCGTAGGTGAACCTGCGG-3';

ITS4 (reverse): 5'-TCCTCCGCTTATTGATATGC-3'.

Phản ứng PCR được thực hiện với tổng thể tích là 50 µL, thành phần mỗi phản ứng bao gồm: 25 µL Green Master Mix 2X, 5 µL mồi ITS 1F (10 pmol), 5 µL mồi ITS 4R (10 pmol), 5µL DNA tổng số (50 ng), 10 µL nước MiliQ. Thực hiện chu trình nhiệt: 95^0C/ 10 phút, tiếp đến là 30 chu kỳ: 95^0C/ 1 phút, 55^0C/ 1 phút, 72^0C/ 1 phút, cuối cùng là 72^0C/ 10 phút. Sản phẩm PCR được xác nhận bằng điện di trên gel agarose 1%, tinh sạch và tiến hành giải trình tự. Các trình tự sau đó được xử lý bằng phần mềm BioEdit và so sánh với các trình tự tương ứng của các chủng đã được đăng ký trên GenBank bằng công cụ BLAST trên NCBI - National Center for Biotechnology Information (www.ncbi.nlm.nih.gov).

Lây nhiễm nhân tạo: Song song, mẫu phân lập đại diện đều được tiến hành lây nhiễm nhân tạo theo quy trình Koch để xác minh lại đối tượng gây hại. Cây sen 20 ngày tuổi được tiến hành gây bệnh nhân tạo bằng cách gây tổn thương bề mặt lá, tiêm dịch nuôi cấy mẫu nấm vào vị trí vết thương, cây đối chứng cũng được xử lý tương tự nhưng thay dịch nấm bằng nước cất. Sử dụng màng nylon bao bọc kín vị trí lây bệnh. Kiểm tra và so sánh những lá sen được lây bệnh với những lá đối chứng. Quan sát và ghi nhận các triệu chứng sau khi lây nhiễm, so sánh với các triệu chứng quan sát được trên đồng ruộng và mẫu bệnh phân lập ban đầu.

Phương pháp xác định ảnh hưởng của vật liệu nano bạc với nấm bệnh *Curvularia lunata*

Cắt một mảnh nấm thuần có kích thước 2 × 2 mm từ rìa của tản nấm sau 48 giờ nuôi cấy ở 28°C, đặt vào tâm các đĩa petri (Φ 9cm) môi trường PDA với nano bạc ở các nồng độ tương ứng khác nhau (0 ppm - đối chứng, 0,1 mg/L, 1 mg/L, 10 mg/L, 20 mg/L, 30 mg/L), rồi tiến hành nuôi cấy ở cùng nhiệt độ. Mỗi nồng độ khảo sát được lặp lại 3 lần. Sử dụng thước kẹp điện tử để đo đường kính tản nấm sau 72 giờ và 96 giờ.

Hiệu lực ức chế của vật liệu nano bạc với nấm được tính theo công thức của Abbott*:*

$$HLUC(\%) = \frac{C - T}{C} x100$$

Trong đó: HLUC (%): là hiệu lực ức chế của nano bạc tính theo phần trăm, C (mm): đường kính tản nấm trong công thức đối chứng, T (mm): Kích thước tản nấm trong các công thức thí nghiệm xử lý nano bạc

KẾT QUẢ VÀ THẢO LUẬN

Tình hình và triệu chứng bệnh đốm lá trên cây Sen Trắng

Bệnh được ghi nhận vào tháng 5 đến tháng 6 tại ruộng trồng sen (giống Sen Trắng Trẹt Lõm) tại xã Phong Hiền, huyện Phong Điền, tỉnh Thừa Thiên Huế. Diện tích trồng sen có xuất hiện triệu chứng bệnh đốm lá lên đến 30%. Triệu chứng được ghi nhận chủ yếu trên bề mặt lá (xuất hiện ở lá non, lá trưởng thành). Đặc điểm nhận dạng ban đầu là những chấm nhỏ li ti, có dạng hình tròn, gần tròn hoặc bầu dục nhỏ, kích thước vết bệnh khoảng 0,4 - 2,5 mm, trung tâm vết bệnh màu nâu nhạt hoặc nâu, đường rìa bao quanh màu nâu đậm hoặc đỏ. Phần tiếp giáp giữa phần mô bệnh và mô khỏe có quầng vàng bao quanh. Các vết bệnh này có thể gia tăng kích thước theo thời gian, có xu hướng liên kết lại với nhau tạo thành vết bệnh rộng (Hình 1).

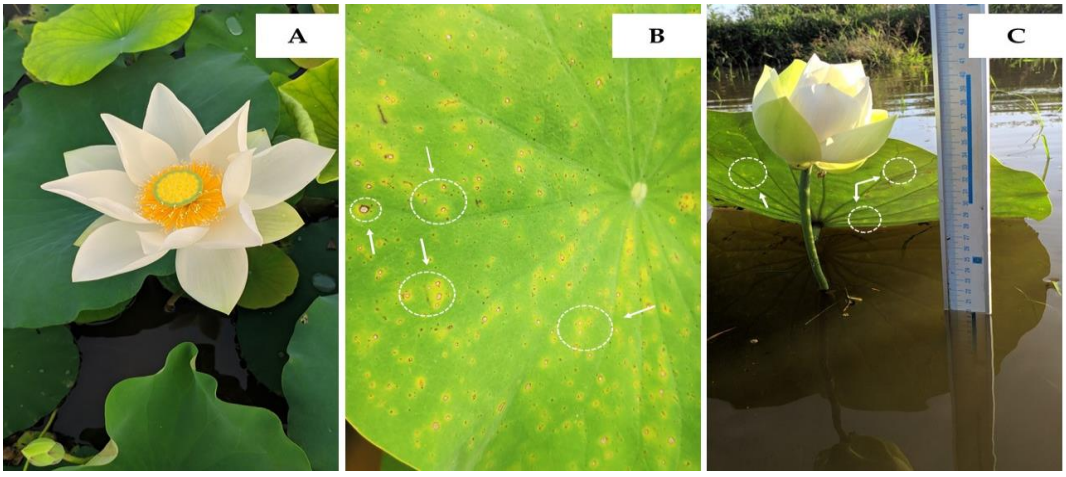

Hình 1. Triệu chứng bệnh đốm lá ghi nhận thực địa tại ruộng trồng sen.
A. Cây Sen Trắng khỏe không nhiễm bệnh;B. Mặt trên lá Sen Trắng nhiễm bệnh đốm lá;
C. Mặt dưới lá với các triệu chứng bệnh đốm lá.

Phân lập và xác định hình thái đối tượng gây bệnh đốm lá ở cây Sen Trắng:

Trên môi trường nuôi cấy PDA ở mẫu nấm bệnh (ký hiệu H3), ở mặt trên, tản nấm ban đầu có màu xám đậm sau chuyển thành màu đen rêu đậm khi già đi (Hình 2), không có dấu hiệu của sự khuếch tán của sắc tố vào môi trường, mặt dưới có màu đen rêu đậm. Quan sát dưới kính hiển vi cho thấy, khuẩn ty mọc thẳng, không phân nhánh, có vách ngăn, uốn nếp ở phần đỉnh. Bào tử có có dạng hình trứng dài-cong nhẹ ở phần dưới, màu nâu ô liu, phần đầu và phần cuối có màu hơi nhạt hơn so với trung tâm, có vách ngăn (3 - 4), cong ở tế bào dưới, kích thước dao động trung bình 20 - 25 µm × 8,5 - 12 µm. Những đặc điểm hình thái này tương tự với những mô tả trước đây về nấm*Curvularia lunata* (Wakker) Boed (Macri và Lenna, 1974). Tiếp theo, kỹ thuật giải trình tự vùng gen ITS được chúng tôi sử dụng để định danh, xác định chính xác tên loài.

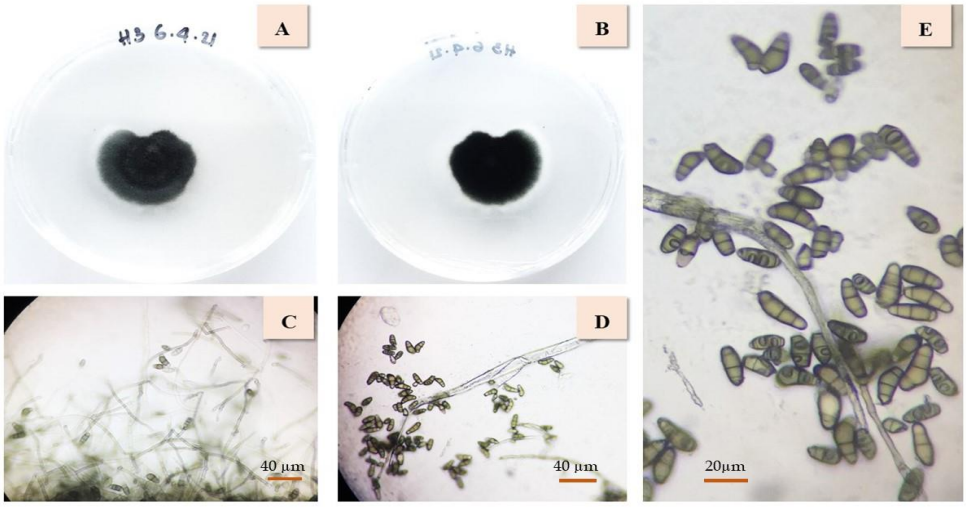

Hình 2. Đặc điểm hình thái của mẫu nấm bệnh H3 trên môi trường PDA.
A: Mặt trên tản nấm sau 3 ngày nuôi cấy; B: Mặt dưới tản nấm sau 3 ngày nuôi cấy;
C, D, E: hình ảnh bào tử nấm dưới kính hiển vi ở các độ phóng đại

Định danh nấm bệnh bằng kỹ thuật sinh học phân tử

Các mẫu nấm sau khi được nhận dạng sơ bộ đặc điểm hình thái, đối chiếu và kiểm tra kết quả lây nhiễm nhân tạo được tiến hành định danh chính xác tên loài dựa vào giải trình tự vùng ITS (internal transcribed spacer). Việc tiến hành tách chiết DNA và PCR nhân đoạn ITS theo mô tả trong phương pháp, kết quả điện di sản phẩm PCR cho thấy mẫu nấm bệnh phân lập (ký hiệu H3) xuất hiện băng rõ nét sản phẩm với kích thước khoảng 550-600 bp (Hình 3) so với thang chuẩn DNA (MK). Điều này phù hợp với các nghiên cứu trước khi sử dụng cặp mồi chung ITS1 và ITS4 để khuếch đại vùng ITS1-5.8S-ITS2 trên các dòng nấm là khoảng 500 - 600 bp.

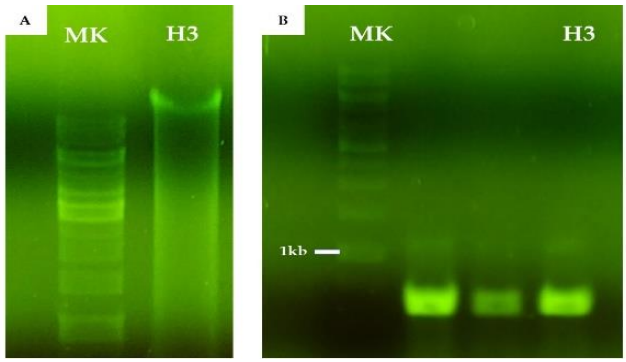

Hình 3. Hình ảnh điện di DNA tổng số và sản phẩm PCR.
A. Hình ảnh điện di DNA tách chiết từ mẫu nấm gây bệnh đốm lá phân lập.
B. Hình ảnh điện di sản phẩm PCR của mẫu nấm gây bệnh đốm lá

Kết quả giải trình tự gen cho thấy mẫu không bị nhiễu và trình tự đọc được có kích thước là 592bp. Trình tự này được tìm kiếm kiếm và so sánh với các chuỗi tương đồng trên Ngân hàng Gen (GenBank) bằng sử dụng phần mềm trực tuyến BLAST của NCBI. Kết quả phân tích BLAST trên GenBank cho thấy trình tự ITS của chủng nấm H3 tương đồng 100% với trình tự vùng ITS của loài nấm *Curvularia lunata* (Accession number: KF924040.1) (Hình 4). Như vậy, kết hợp với các đặc điểm hình thái xác định ở trên, chủng H3 gây bệnh đốm lá trên cây Sen Trắng có thể kết luận đó là nấm *Curvularia lunata.* Những báo cáo ghi nhận về bệnh đốm nâu lá và triệu chứng liên quan do *Curvularia* cũng đã được ghi nhận ở các báo cáo trước đây ở giống lúa IR66 ở Pakistan, Campuchia (Tann, 2016), hay lần đầu tiên ghi nhận trên thanh long ruột đỏ (*Hylocereus polyrhizus*) ở Malaysia [5], sắn (*Manihot esculenta*) ở vùng Tây Phi [6], lúa hoang (*Oryza rufipogon*) ở Trung Quốc [7] và ngô ở Hoa Kỳ [8]. Nghiên cứu của Pei và đồng tác giả (2017) là báo cáo đầu tiên về bệnh đốm lá với những triệu chứng điển hình trên lá ớt (*Capsicum frutescens*) với đối tượng gây hại được xác định là *Curvularia lunata* ở Trung Quốc. *Curvularia lunata* cũng được xác định là đối tượng gây bệnh đốm lá sen khiến 60% diện tích trồng bị nhiễm bệnh tại tỉnh Giang Tây, Trung Quốc trong báo cáo của Cui và Sun năm 2012 [15].

```
Query  301  TTCCGTAGGGGAACCTGCGGAGGGATCATTACACAATAAAATATGAAGGCTGTACGCGGC  360
            ||||||||| ||||||||||||||||||||||||||||||||||||||||||||||||||
Sbjct  2    TTCCGTAGGTGAACCTGCGGAGGGATCATTACACAATAAAATATGAAGGCTGTACGCGGC  61

Query  361  TGTGCTCTCGGGCCAGTTTTGCGGAGGCTGAATTATTTATTACCCTTGTCTTTTGCGCAC  420
            ||||||||||||||||||||||||||||||||||||||||||||||||||||||||||||
Sbjct  62   TGTGCTCTCGGGCCAGTTTTGCGGAGGCTGAATTATTTATTACCCTTGTCTTTTGCGCAC  121

Query  421  TTGTTGTTTCCTGGGCGGGTTCGCCCGCCACCAGGACCACATCATAAACCTTTTTTATGC  480
            ||||||||||||||||||||||||||||||||||||||||||||||||||||||||||||
Sbjct  122  TTGTTGTTTCCTGGGCGGGTTCGCCCGCCACCAGGACCACATCATAAACCTTTTTTATGC  181

Query  481  AGTTGCAATCAGCGTCAGTATAACAAATGTAAATCATTTACAACTTTCAACAACGGATCT  540
            ||||||||||||||||||||||||||||||||||||||||||||||||||||||||||||
Sbjct  182  AGTTGCAATCAGCGTCAGTATAACAAATGTAAATCATTTACAACTTTCAACAACGGATCT  241

Query  541  CTTGGTTCTGGCATCGATGAAGAACGCAGCGAAATGCGATACGTAGTGTGAATTGCAGAA  600
            ||||||||||||||||||||||||||||||||||||||||||||||||||||||||||||
Sbjct  242  CTTGGTTCTGGCATCGATGAAGAACGCAGCGAAATGCGATACGTAGTGTGAATTGCAGAA  301

Query  601  TTCAGTGAATCATCGAATCTTTGAACGCACATTGCGCCCTTTGGTATTCCAAAGGGCATG  660
            ||||||||||||||||||||||||||||||||||||||||||||||||||||||||||||
Sbjct  302  TTCAGTGAATCATCGAATCTTTGAACGCACATTGCGCCCTTTGGTATTCCAAAGGGCATG  361

Query  661  CCTGTTCGAGCGTCATTTGTACCCTCAAGCTTTGCTTGGTGTTGGGCGTTTTTTGTCTTT  720
            ||||||||||||||||||||||||||||||||||||||||||||||||||||||||||||
Sbjct  362  CCTGTTCGAGCGTCATTTGTACCCTCAAGCTTTGCTTGGTGTTGGGCGTTTTTTGTCTTT  421

Query  721  GGTTGCCAAAGACTCGCCTTAAAAGGATTGGCAGCCGGCCTACTGGTTTCGCAGCGCAGC  780
            ||||||||||||||||||||||||||||||||||||||||||||||||||||||||||||
Sbjct  422  GGTTGCCAAAGACTCGCCTTAAAAGGATTGGCAGCCGGCCTACTGGTTTCGCAGCGCAGC  481

Query  781  ACATTTTTGCGCTTGCAATCAGCAAAAGAGGACGGCAATCCATCAAGACTCCTTCTCACG  840
            ||||||||||||||||||||||||||||||||||||||||||||||||||||||||||||
Sbjct  482  ACATTTTTGCGCTTGCAATCAGCAAAAGAGGACGGCAATCCATCAAGACTCCTTCTCACG  541

Query  841  TTTGACCTCGGATCAGGTAGGGATACCCGCTGAACTTAAGCATATCAATAA  891
            ||||||||||||||||||||||||||||||||||||||||||||||||||
Sbjct  542  TTTGACCTCGGATCAGGTAGGGATACCCGCTGAACTTAAGCATATCAATAA  592
```

Hình 4. Mức độ tương đồng giữa mẫu nấm bệnh H3 với trình tự đã được công bố trên GeneBank (Mã số: KF924040.1)

Lây nhiễm nhân tạo

Quá trình lây nhiễm nhân tạo được tiến hành trên cây sen khỏe để kiểm tra xác minh tác nhân gây bệnh phân lập được. Cây sen khỏe được gây tổn thương bề mặt nhân tạo. Dịch bào tử chứa 3 x 10^5 bào tử/mL được lây nhiễm lên vết thương. Cây đối chứng được xử lý bằng nước cất tại vị trí lá gây tổn thương. Kết quả cho thấy, sau 5 ngày, tại vị trí vết bệnh xuất hiện những chấm tròn nhỏ bao quanh quầng vàng. Các đặc điểm này tương tự với triệu chứng bệnh điển hình thu nhận tại tự nhiên (Hình 5). Cây đối chứng xử lý bằng nước cất không có dấu hiệu bệnh tại vị trí gây tổn thương (Hình 5.E). Sự tương đồng về hình thái, triệu chứng vết bệnh trên lá sen khỏe lây nhiễm nhân tạo với kết quả ghi nhận bệnh đốm trắng ở điều kiện tự nhiên, có thể kết luận chủng nấm H3 - *Curvularia lunata* là đối tượng gây bệnh đốm lá trên cây Sen Trắng.

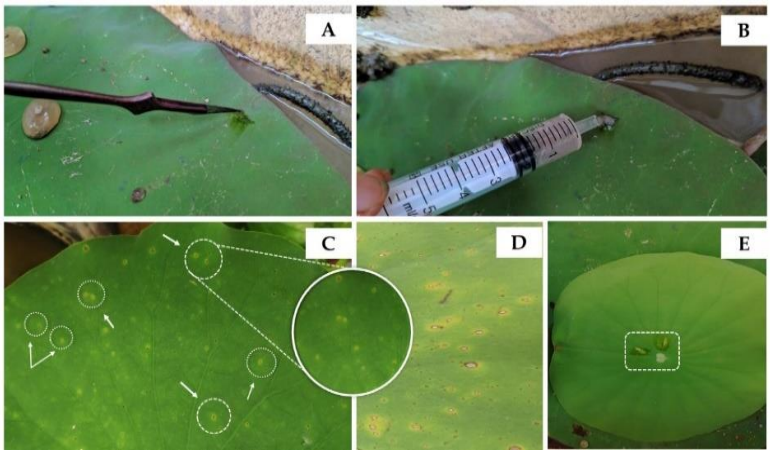

Hình 5. Tiến hành lây nhiễm nhân tạo (quy trình Koch).

A, B. Tiến hành gây tổn thương bề mặt và tiến hành lây nhiễm;
C. Cây sen khỏe xuất hiện triệu chứng bệnh điển hình;
D. Đối chiếu vết bệnh tại tự nhiên;
E. Cây đối chứng không có biểu hiện bệnh

Thử nghiệm hoạt tính kháng nấm *Curvularia lunata* của vật liệu nano bạc trong điều kiện *in vitro*

Trong nghiên cứu này, chúng tôi thực hiện thử nghiệm hoạt tính ức chế sự phát triển của nấm bệnh *Curvularia lunata* bằng vật liệu nano bạc. 5 nồng độ nano bạc tăng dần từ 0,1 mg/L, 1 mg/L, 10mg/L, 20mg/L và 30mg/L được sử dụng để tiến hành khảo sát và 0 mg/L được sử dụng như mẫu đối chứng (control). Kết quả thu được cho thấy, đường kính sinh trưởng của tản nấm *Curvularia lunata*trên môi trường PDA giảm dần tương ứng với gia tăng nồng độ nano bạc, đồng nghĩa hiệu lực ức chế nấm tăng dần tương ứng với sự gia tăng nồng độ nano bạc. Cụ thể, với sự có mặt của nano bạc ở nồng độ 20mg/L cho thấy hiệu lực ức chế lên đến hơn 60%, với 68,32% và 61,47% tương ứng sau 3 ngày và 5 ngày thử nghiệm. Sự có mặt nano bạc ở nồng độ cao 30 mg/L có hiệu lực ức chế đáng kể đến nấm *Curvularia lunata,* với hiệu lực là 91,37% sau 3 ngày và 93,21% sau 5 ngày. Những kết quả này phù hợp với những kết quả thu được của Huang et al. (2018), các tác giả sử dụng vật liệu nano bạc bằng phương pháp tổng hợp "xanh", với chiết xuất lá của cây Hoàng dương Nhật Bản (*Buxus sinica*) được sử dụng như tác nhân khử với $AgNO_3$ 4mM để thử nghiệm hoạt tính kháng nấm *Curvularia lunata*. Kết quả cho thấy ở nồng độ 200 µg/mL ức chế sự phát triển lên đến 85% và giá trị IC_{50} đạt 26 µg/mL, hình thái sợi nấm cũng bị biến dạng khi được xử lý với nano bạc [9]. Trong nghiên cứu gần đây của Uz-Zamam et al. (2020), tác giả đã tiến hành thử nghiệm hoạt tính kháng nấm trên các đối tượng *Alternaria alternata, Paecilomyces, Candida albicans, Curvularia, Aspergilus niger*, và *Rhizopus* với hiệu quả thu được lần tương ứng lần lượt là 54,05%, 42,11%,41,10%, 40.85%, 30,55%, và 29,73% với nano bạc được tổng hợp từ chiết xuất củ *Trillium govanianum* Wall. Ex. Royle đóng vai trò là chất khử, chất ổn định để khử bạc nitrat [10]. Khả năng kháng nấm của vật liệu nano bạc với hiệu lực ức chế đáng kể đến nấm gây bệnh thực vật như *Bipolaris sorokiniana, Colletotrichum, Fusarium* sp., *Penicillium* sp cũng đã được báo cáo trong các nghiên cứu của Azarbani và đồng tác giả, Dutta và đồng tác giả [11, 12].

Bảng 1. Khảo sát hiệu lực ức chế của vật liệu nano bạc với nấm *C. lunata* ở các nồng độ khác nhau

		Control	0.1 mg/L	1 mg/L	10 mg/L	20 mg/L	30 mg/L
Sau 3 ngày	**Đường kính tản nấm (mm)**	35,2	31,48 ± 0,08	23,92 ± 0,28	19,03 ± 0,16	11,15 ± 0,15	3,04 ± 0,06
	Hiệu lực ức chế (%)	0	10,56 ± 0,22	32,05 ± 0,78	45,92 ± 0,46	68,32 ± 0,42	91,37 ± 0,16

		Control	0.1 mg/L	1 mg/L	10 mg/L	20 mg/L	30 mg/L
Sau 5 ngày	**Đường kính tản nấm (mm)**	48,6	45,10 ± 0,56	38,13 ± 0,32	26,08 ± 0,07	18,73 ± 0,21	3,30 ± 0,26
	Hiệu lực ức chế (%)	0	7,20 ± 1,14	21,54 ± 0,66	46,33 ± 0,16	61,47 ± 0.42	93,21 ± 0,54

Khả năng kháng nấm của vật liệu nano bạc có được ở nồng độ cao có thể là do ở nồng độ đó, dung dịch nano bạc có khả năng bão hòa và bám vào các sợi nấm và để kiểm soát các bệnh thực vật. Feng và cộng sự nhận thấy rằng DNA mất khả năng nhân đôi khi môi trường nuôi cấy nấm được xử lý bằng nano bạc [13]. Điều này có thể dẫn đến sự vô hiệu hoá biểu hiện các protein tiểu đơn vị của ribosome, làm gián đoạn quá trình tổng hợp các enzyme và protein quan trọng đối với việc sản xuất adenosine triphosphate. Nghiên cứu của Bragg và Rainnie đưa ra giả thuyết rằng các ion bạc chủ yếu ảnh hưởng đến chức năng của các enzyme liên kết màng, phá vỡ cấu trúc màng, ví dụ như các enzyme trong chuỗi hô hấp [14]. Những cơ sở khoa học này và kết quả nghiên cứu chúng tôi thực hiện, vật liệu nano bạc (AgNPs) có thể được xem như giải pháp tiềm năng để xử lý nấm *Curvularia lunata* gây hại trên cây Sen Trắng và các nấm bệnh thực vật nói chung.

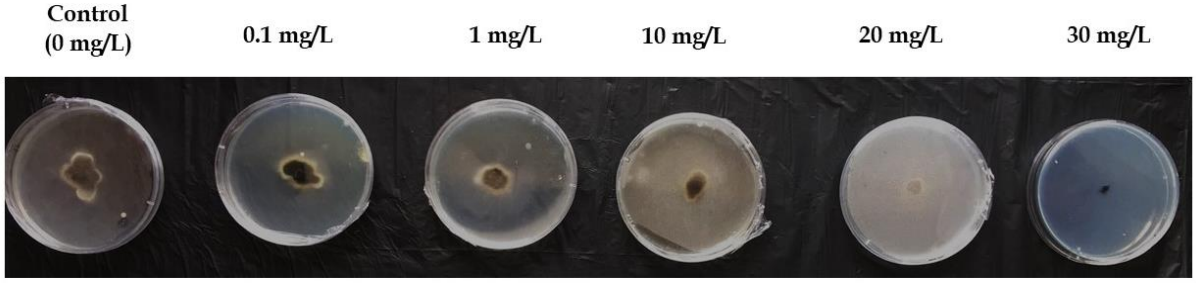

Hình 6. Hiệu lực ức chế của vật liệu nano bạc ở các nồng độ tương ứng sau 72 giờ (3 ngày)

KẾT LUẬN

Trong nghiên cứu này, chúng tôi đã phân lập và định danh bằng hình thái và phân tử đối tượng gây bệnh đốm lá trên cây Sen Trắng trồng tại Thừa Thiên Huế vụ mùa 2021 là *Curvularia lunata* bằng cách sử dụng cặp primer ITS1-ITS4 với độ tương đồng 100%. Theo hiểu biết của chúng tôi, đây là báo cáo đầu tiên về *Curvularia lunata* gây ra bệnh đốm lá trên cây Sen Trắng *Nelumbo nucifera* ở Việt Nam. Bên cạnh đó, xử lý nano bạc ở nồng độ 30 mg/L cho thấy hiệu quả tích cực với hiệu lực ức chế nấm *Curvularia lunata* lên đến 91,37% và 93,21% tương ứng sau 72 giờ (3 ngày) và 120 giờ (5 ngày) so với đối chứng không xử lý.

Lời cảm ơn: *"Nguyễn Quang Hoàng Vũ được tài trợ bởi Tập đoàn Vingroup và hỗ trợ bởi chương trình học bổng đào tạo Thạc sĩ, Tiến sĩ trong nước của Quỹ Đổi mới sáng tạo Vingroup (*VINIF*), Viện Nghiên cứu Dữ liệu lớn (VinBigdata), mã số [VINIF.2020.TS.89]"*

TÀI LIỆU THAM KHẢO

[1] N. T. Q. Trang," *Nghiên cứu đặc điểm thực vật học, sinh lý hóa sinh và nhân giống invitro một số giống sen (Nelumbo nucifera* Gaertn*.) trồng ở Thừa Thiên Huế*. Luận án Tiến sĩ, Đại học Khoa học Huế, 2021**.**

[2] K. Kalwar and D. Shan, "Antimicrobial effect of silver nanoparticles (AgNPs) and their mechanism - A mini Review," *Micro and Nano Letters*, Vol. 13, No. 3. 2018.

[3] L. W. Burgess, T. E. Knight, T. Len, and P.H. Thuy, "Diagnostic manual for plant diseases in Vietnam," *Aust. Cent. Int. Agric. Res*., 2008.

[4] J. J. Doyle and J. L. Doyle, "A rapid DNA isolation procedure for small quantities of fresh leaf tissue," *Phytochem. Bulletin*, Vol. 19, pp. 11-15, 1987.

[5] M. M. Hawa, B. Salleh, and Z. Latiffah, "First report of *Curvularia lunata* on red-fleshed dragon fruit (*Hylocereus polyrhizus*) in Malaysia," *Plant Disease*, Vol. 93, No. 9, 2009.

[6] W. Msikita, H. Baimey, and B. D. James, "Severity of Curvularia stem blight disease of cassava in West Africa," *Plant Disease.*, Vol. 91, no. 11, pp. 1430-1435, 2007.

[7] H. K. Zhou, Y.L. Liu, J. R. Tang, et al., "First Report of Leaf Spot caused by *Curvularia lunata* on Wild Rice in China", *Plant Disease*, 2021.

[8] T. Garcia-Aroca, V. Doyle, R. Singh, et al., "First report of *Curvularia* leaf spot of corn, caused by *Curvularia lunata*, in the United States," *Plant Health Progress*, Vol. 19, No. 2, 2018.

[9] R. Q. Cui and X. T. Sun, "First report of curvularia lunata causing leaf spot on lotus in China," *Plant Disease*, Vol. 96, No.7, 2012

[10] K. Uz-Zaman, J. Bakht, B. Kudaibergenova et al., "*Trillium govanianum* Wall. Ex. Royle rhizomes extract-medicated silver nanoparticles and their antimicrobial activity," Green Processing and Synthesis, Vol. 9, No. 1, 2020.

[11] T. Dutta, S. K. Chowdhury, N.N. Ghosh, et al., "Journal of environmental chemical engineering greensynthesis of antibacterial and antifungal silver nanoparticles using *Citrus limetta* peel extract : Experimental and theoretical studies", *Journal of Environmental Chemical Engineering*, Vol. 8, No. 4, pp. 1-16, 2020.

[12] F. Azarbani and S. Shiravand, "Green synthesis of silver nanoparticles by *Ferulago macrocarpa* flowers extract and their antibacterial, antifungal and toxic effects," *Green Chemistry Letters and Reviews*, Vol. 13, No. 1. 2020.

[13] Q. L. Feng, J. Wu, G. Q. Chen et al., "A mechanistic study of the antibacterial effect of silver ions on *Escherichia coli* and *Staphylococcus aureus*". *Biomedical Materials Research*, Vol.52, pp.662-668, 2000**.**

[14] P. D. Bragg and D. J. Rainnie, "The effect of silver ions on the respiratory chain of *Escherichia coli*," **Canadian Journal of Microbiology**, Vol. 20, No. 6,pp. 883 -889, 1974.

[15] W. Huang, Y. Bao, H. Duan, Y. Bi et al., "Antifungal effect of Buxus sinica leaf extract-mediated silver nanoparticles against *Curvularia lunata*", *International Journal of Agriculture And Biology*, Vol. 20, No. 11, 2018.

ANTIFUNGAL ACTIVITY OF SILVER NANOPARTICLES AGAINST*CURVULARIA LUNATA* CAUSING LEAF SPOT ON WHITE LOTUS (*NELUMBO NUCIFERA*) IN THUA THIEN HUE

Nguyen Quang Hoang Vu[1], Hoang Tan Quang[1], Hoang Thi Kim Hong[2*]

[1]*Institute of Biotechnology, Hue University*

[2]*Department of Biology, Hue University of Sciences, Hue University*

SUMMARY

This study was conducted to isolate and identify plant fungal pathogen from leaf spot disease on white lotus cv. (*Nelumbo nucifera*) in Thua Thien Hue.The colonies of the isolates on PDA were initially light gray later becoming dark green. Conidiophores were erect, dark brown, geniculate, and unbranched. Conidia were oval or hook-shaped, smooth-walled, dark-brown, 3-4 septate, with cells about 20-25 µm × 6.5-12 µm in size. Molecular identification of strain using primer pairs ITS1, ITS4 showed that *Curvularia lunata* were the fungal pathogen. To our knowledge, this is the first report on *Curvularia lunata* causing leaf spots on lotus (*Nelumbo nucifera*) in Vietnam. In this study, we have evaluated the antifungal activity of silver nanoparticles (AgNPs) against *Curvularia lunata*. Fungicidal activity of silver nanoparticle at different concentration: 0.1 mg/L, 1 mg/L, 10 mg/L, 20 mg /L, 30 mg/L tested against fungal. Radial fungal growth was recorded after 3 and 5 days. Different concentrations of AgNPs inhibit colony formation of *C. lunata* at different levels. As the concentration of AgNPs was increased, there was a decrease in colony formation. At 20 mg/L, the silver nanoparticles inhibited the fungus *Curvularia lunata* up to 68.32% and 61.47% at 3 days and 5 days, respectively. The application of 30 mg/L concentration of silver nanoparticles produced maximum inhibition of the growth of fungal hyphae, with 91.37% and 93.21%. Thus, silver nanoparticles are effective in inhibiting the growth of Curvularia *lunata* and these findings may suggest silver nanoparticles (AgNPs) as a green solution with potent antifungal activities against plant pathogenic fungi.

Keywords: leaf spots, *Curvularia lunata*, antifungal, silver nanoparticles, *Nelumbo nucifera*, Thua Thien Hue, white lotus

[*]Author for correspondence: Tel: +84-978 939 467; Email: hkhong@hueuni.edu.vn

Microbiology Associated with Disease on White Lotus (Nelumbo nucifera Gaertn.) and Application of Silver Nanoparticles for the Control of Plant Pathogens In vitro

VU, Nguyen Quang Hoang
Institute of Biotechnology, Hue University

QUANG, Hoang Tan
Institute of Biotechnology, Hue University

HONG, Hoang Thi Kim
Duy Tan University, Da Nang City

AGARIE, Sakae
Laboratory of Plant Production Physiology, Division of Agrobiological Science, Department of Bioresource Sciences, Faculty of Agriculture, Kyushu University

出版情報：九州大学大学院農学研究院紀要. 67 (2), pp.165-172, 2022-09. Faculty of Agriculture, Kyushu University
バージョン：
権利関係：

J. Fac. Agr., Kyushu Univ., **67** (2), 165–172 (2022)

Microbiology Associated with Disease on White Lotus (*Nelumbo nucifera* Gaertn.) and Application of Silver Nanoparticles for the Control of Plant Pathogens *In vitro*

Nguyen Quang Hoang VU[1], Hoang Tan QUANG[1], Hoang Thi Kim HONG[2]* and Sakae AGARIE

Laboratory of Plant Production Physiology, Division of Agrobiological Science,
Department of Bioresource Sciences, Faculty of Agriculture,
Kyushu University, Fukuoka 819–0395, Japan
(*Received May 8, 2022 and accepted May 10, 2022*)

Many bacterial and fungal pathogens are known to affect lotus, which limits both flower quality and yield production. Treatments such as pesticides can reduce pathogens but can result in resistance. This study was conducted to identify the most common fungal, and bacterial pathogens associated with leaf spot diseases of white lotus (*Nelumbo nucifera*). Molecular–based identification using ITS and 16 s ribosomal DNA sequences revealed that the isolates belonged to *Aspergillus aculeatus*, *Aspergillus fumigatus*, and *Klebsiella pneumoniae*. We evaluated the effect of silver nanoparticles against pathogens isolated from infected white lotus leaves. According to the findings, AgNPs have antifungal activities against these plant diseases at different concentrations of 0.1,1, 10, 20, and 30 mg/L. Treatment of 30 mg/L silver nanoparticles on PDA showed the highest inhibition rate of plant pathogenic fungi *Aspergillus* sp., and bacteria *Klebsiella pneumoniae*. Based on this result, it is possible to suggest that silver nanoparticles synthesized could be an efficient, safe, cost–effective, and affordable alternative to control disease in white lotus.

Key words: silver nanoparticles, antifungal, antibacterial, white lotus, pathogen plant

INTRODUCTION

Lotus (*Nelumbo nucifera* Gaertn.) is a potential perennial aquatic crop grown and consumed throughout Asia. The lotus plant is a symbol of purity in many countries. All parts of *N. nucifera* have been used for multiple purposes, such as food, ornamental, and herbal medicinal products (Zhu, 2017). Besides, it is particularly noted for its 1,300–year seed longevity. In particular, among the lotus cultivars, the white lotus is a traditional indigenous variety. It has a characteristic floral aroma, and its seeds are sweet, fleshy, and sticky. However, due to the competition of high–yielding lotus "Cao san" varieties and harmful pathogens appearing in lotus fields, the planting area gradually shrinks, leading to the risk of degeneration and loss of varieties.

Many bacterial and fungal pathogens affect lotus, limiting both lotus flower quality and plant yield production. Synthetic chemical fungicides and pesticides have been the most commonly applied method to control lotus diseases. However, the extensive use of fungicides and pesticides is causing environmental pollution (soil, water). These practices may have a harmful influence on beneficial non–target species in the ecosystem and negatively affect the biodiversity, contributing to the development of resistant pathogens, possibly posing a potential risk to human health, and threatening the food security of humans on this planet (Bartlett *et al.*, 2002). Therefore, there is a growing need to develop alternative approaches to control plant diseases. Recently, nanotechnology has drawn attention due to its numerous applications in health, pharmaceuticals, catalysis, energy, environmental sciences, and materials (Rajashekara, 2012). The metal nanoparticles demonstrated distinct and significantly different physical and chemical characteristics (Feldheim and Foss, 2002). This is true especially in regards to silver nanoparticles (AgNPs) with their large surface area which makes them attractive to addressing the challenges not met by the physical, chemical pesticides, and other biological control methods methods (Pulimi and Subramanian, 2016). Therefore, they have the potential to be widely used in agriculture as biocontrol agents to promote sustainable agriculture (Franci *et al.*, 2015; Rajwadi *et al.*, 2020).

The objectives of this study were to isolate and identify plant pathogens from the lake–grown white lotus regions and investigate the antifungal, antibacterial effect of green synthesized silver nanoparticles (AgNPs) to control lotus (*N. nucifera*) disease.

MATERIALS AND METHODS

Silver nanoparticles

A stock solution of silver nanoparticles (AgNPs) at a 40 mg/L (ppm) concentration was synthesized using green *Aloe barbadensis*. The synthesis of AgNPs using leaf extracts was done using the method described previously (Hong *et al.*, 2021). Solution contain different AgNPs were added to growth media to make different AgNPs concentrations (0.1, 1, 10, 20, 30 mg/L). All silver nanoparticle solutions and media were freshly prepared and used.

Collection of samples

From March to May 2021, lesion leaves were col-

[1] Institute of Biotechnology, Hue University, Vietnam
[2] Duy Tan University, Da Nang City, Vietnam
* Corresponding author: (E–mail: hoangtkimhong@duytan.edu.vn)

lected randomly, transported to the laboratory within a cooler, and then kept at 4°C until further use.

Fungal and bacterial pathogen isolation

Infected leaf lesions were cut into small pieces (5 × 5 mm) and sterilized with 1% sodium hypochlorite (NaClO) solution for 1 minute. The samples were washed three times with sterilized distilled water, then dried on sterile paper towels, plated on potato dextrose agar (PDA) medium (38 g PDA in 1 L distilled water), and incubated at 28 ± 2°C under 12 h photoperiod for 7 days. Pure cultures were obtained by transferring single hyphal tips to fresh PDA plates. Pure colonies were maintained in 70% glycerol solution and stored at –20°C.

Identification morphological of the fungal and bacterial isolates

The fungal isolates were used to identify their morphology, such as conidiophores, conidia's shape and size, and colony characters.

The morphological characteristics of bacterial isolates were analyzed for their microscopic features (Colour, shape, margin, transparency) through the Gram staining technique as described in Bergey's manual of systematic bacteriology.

Molecular identification of the fungal and bacterial isolates

The total DNA of isolates was extracted from infected leaves using the cetyltrimethyl ammonium bromide (CTAB) method for the PCR performance (Namba *et al*., 1993). The molecular identity of the fungal and bacterial isolate was determined using Polymerase chain reaction (PCR) amplification.

Fungal: The internal transcribed spacer (ITS) region of the ribosomal DNA was amplified and sequenced using primers

+ ITS1F (5'TCCGTAGGTGAACCTGCGG–3') and

+ ITS4 (5'–TCCTCCGCTTATTGATATGC–3') (White *et al*., 1990).

The ITS primers used were ITS–1F and ITS–4. The PCR amplification program consisted of 95°C for 5 min, followed by 35 cycles of 95°C for 1 min, 52°C for 30 seconds, 72°C for 1 min, and a final extension temperature of 72°C for 10 min, holding the temperature of 4°C.

Bacterial: 16sRNA amplification was performed using the primers

+ 27F (5'– AGAGTTTGATCCTGGCTCAG – 3') and

+ 1492R (5'–TACCTTGTTACGACTT–3').

PCR reaction was performed in a Thermal Cycler (Eppendorf, Germany), and the thermal program used for the PCR (polymerase chain reaction) was under the following conditions: initial denaturation at 92°C for 2 *min*, followed by 35 cycles with final denaturation at 92°*C* for 1 min, primer annealing at 50°*C* for 30 seconds, extension at 72°*C* for 90 seconds, and an additional 10 min at 72°C as a final extension. In addition, PCR product was subjected to electrophoresis on 1.2% (*w/v*) agarose gels in 1×TAE Buffer.

The sequences obtained were edited using the BioEdit 7.0 software, and consensus sequences were analyzed using the Molecular Evolutionary Genetics Analysis (MEGA X) software (Kumar *et al*., 2018). The similarity of the nucleotide sequences of the isolate was calculated using the BLAST algorithm (Basic Local Alignment Search Tool).

Pathogenicity test

The pathogenicity of purified isolates from the disease leaves lotus was tested on a concave white lotus and confirmed by Koch's postulates. Lotus were grown in pots under greenhouse conditions. Leaves of plant hosts were sprayed with spore suspensions of each of the isolates using a hand sprayer. Inoculated plants were then kept in a humid chamber and observed daily for disease symptoms

Evaluation of the antibacterial and antifungal activity of silver nanoparticles in the *in vitro*

An *in vitro* assay was carried out on PDA with 0.1, 1, 10, 20, and 30 mg/L of silver nanoparticles (AgNPs). Medium containing silver nanoparticles was poured into each 90 × 15 mm Petri dish. The media containing silver nanoparticles was incubated at room temperature. After 48 hours of incubation, an agar plug of 8 mm diameter containing fungi was inoculated simultaneously at the center of each Petri dish and incubated at 28 ± 2°C. The culture medium without silver nanoparticles was inoculated and cultured under the same conditions for the control treatment. The sizes of the colonies were measured after 5 days and each treatment was replicated.

The inhibition rate – IR (%) was calculated using the following formula: where R is the radial growth of fungi in the control plate, and r is the radial growth of fungi in silver nanoparticle treated plates.

$$IR = \frac{R-r}{R}\ x100$$

Antibacterial potency of synthesized AgNPs for inhibiting the growth of pathogens was tested *in vitro* on LB medium using the agar well–diffusion assay according to Bakht *et al*. (2011). The bacteria strains were spread on the LB medium. The disks were loaded with 50 μL of silver nanoparticles (0.1, 1, 10, 20, and 30 mg/L). The disks were then placed on the agar plate and incubated at 37°C for 24 h. The zone of inhibition was observed after 24 h of incubation. Three replicates were set at 30 ± 2°C.

RESULT AND DISCUSSION

Characteristics of concave white lotus

Concave white lotus was cultivated from mid–February 2021 to August 2021. Different stages of concave white lotus were observed in the field and photographed (Fig. 1). Concave white lotus has a medium–small tree size; young leaves are light green. Flower buds were white to pale green, oval long – shaped, seed pots flat. Lotus seed is elliptical. The pigment inside the

seed coat is white. The diameter of the leaves of white lotus is smaller than other lotus variety

The growth and development of the white lotus variety consists of the following main stages. There are two types of leaves in the vegetative phase: floating leaves and standing leaves. The floating leaf stage (S1) is the initial stage of development for the white lotus plant. When the floating leaves have covered most of the water's surface, the plant begins to generate standing leaves (S2). Following that, buds appear (S3) marking the beginning of the reproductive stage (50 – 60 days after planting). In early and mid–May, blooming starts (S4, S5 – approximately 65 – 75 days after planting). In late May and late June, they reach full bloom (90 – 120 days of planting). The last flowering period starts in mid–July (142 – 155 days). After 170 – 180 days (S8), their leaves turn yellow and wither, and the plant enters dormancy, seed pod has turned green. The seed pod will dry up and turn brown (S10). The entire growth period is 190 to 195 days.

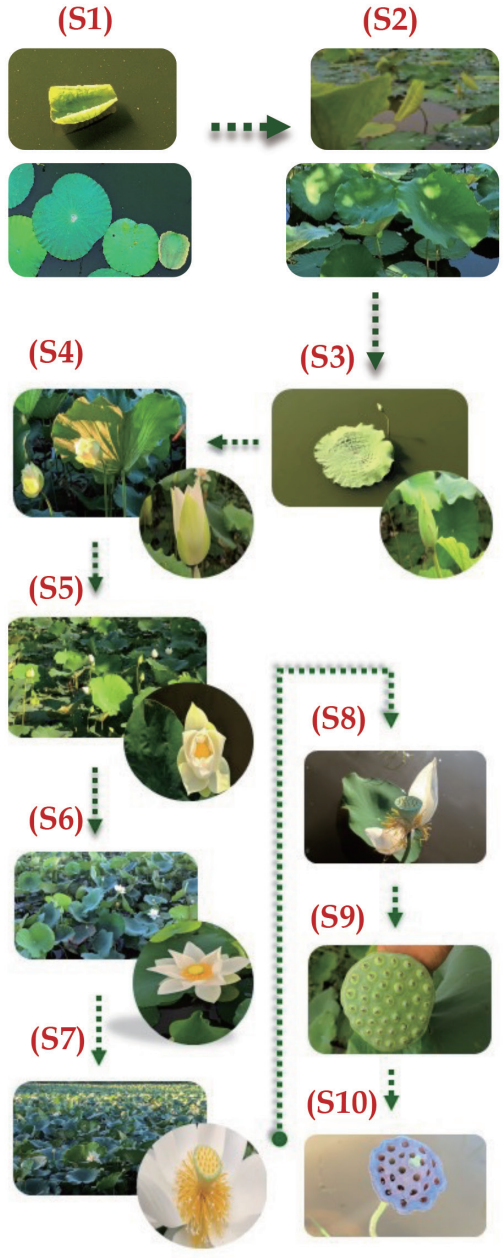

Fig. 1. Morphological, and physiological of concave white lotus (*Nelumbo nucifera*).
S1: floating leaf stage; S2: standing leaf stage; S3: bud appear; S4, S5, S6: Flower blooming; S7: Full bloom; S8: Petal begin fallen; S9: Seed pod has turned green and development; S10: Seed pod turns brown.

Disease symptoms, isolation and identification of the fungal, bacterial pathogen

Necrotic Brown Leaf disease with characteristic symptoms was represented by light brown, canker lesions that spread quickly. The initial stage of the blister blight infection process was marked by brown translucent spots with a yellow halo zone on the upper surface of leaves. At the end of the infection process, necrotic lesions on the leaves were observed. After 5 days, a colony of about 6.5 to 7.2 cm in diameter of STM1 isolates appeared on PDA, and it was brownish–black at the center and white at the edges (Fig. 2 D, E). Radial growth was 72.3 mm (recorded 5 days after injection on PDA). The conidiophore appeared pale brown, and the vesicles were not separate when observed through the microscope.

Brown leaf spot disease with typical symptoms consisted of small yellowish–brown spots, turning to dark brown or black after 7 –10 days infected. Lesion shapes tended to form radial streaks, from specks that became streaks running parallel to the leaf veins. For STM3 isolate from infected leaf (Fig. 3A), observed under the microscope, the isolate was characterized by green *Echinulate conidia*. Radial growth was 67.2 mm (recorded 5 days after injection on PDA). The mycelium differentiated into the septum branched and spore–

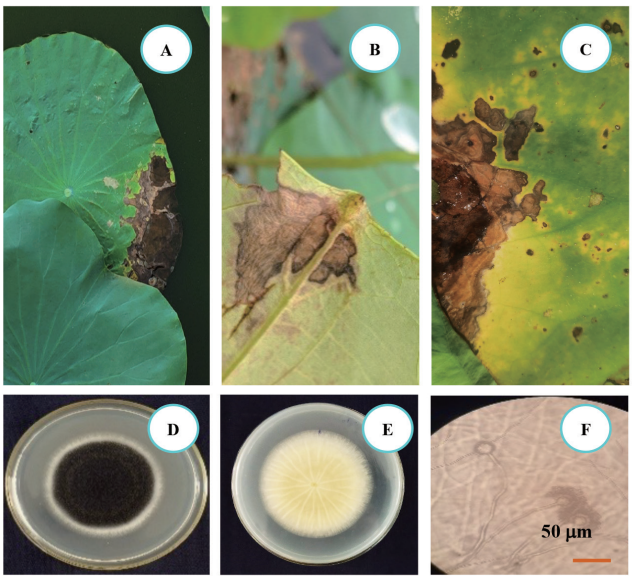

Fig. 2. Symptoms of Necrotic brown spot and pathogen isolate STCM1 (A), (B), (C): Disease symptoms of Necrotic Brown Spot observed in the lake; (D), (E): Colony morphology of STM1 on PDA, (F): Morphology of STCM1 in the microscope. Scale bar = 50 μm.

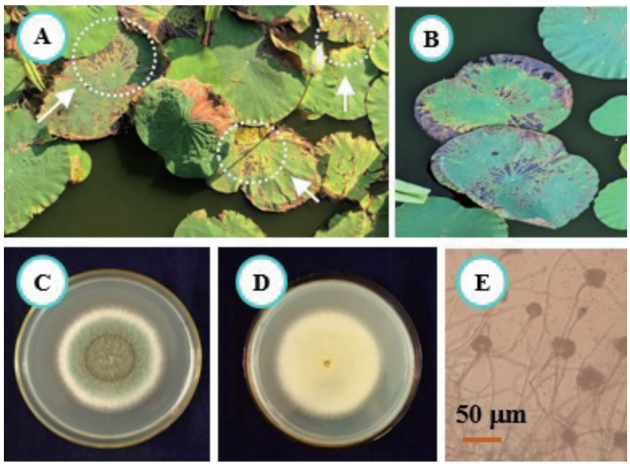

Fig. 3. Disease symptoms of Brown leaf spot and pathogen isolate STCM3
(A), (B): Disease symptoms of Brown leaf spot observed in the lake;
(C), (D): Colony morphology of STCM3 on PDA,
(F): Morphology of STCM3 in the microscope. Scale bar = 50 μm.

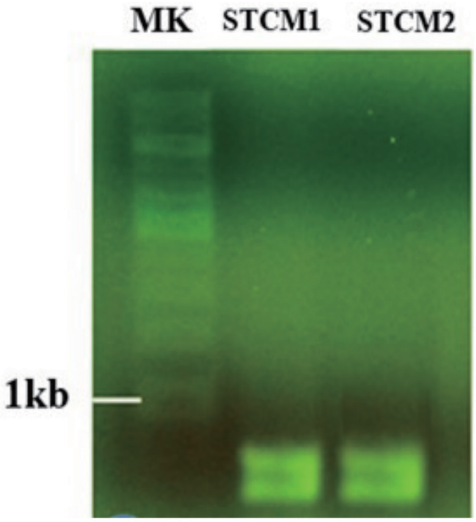

Fig. 4. Electrophoresis DNA total of STCM1, STCM3 isolate. MK: marker.

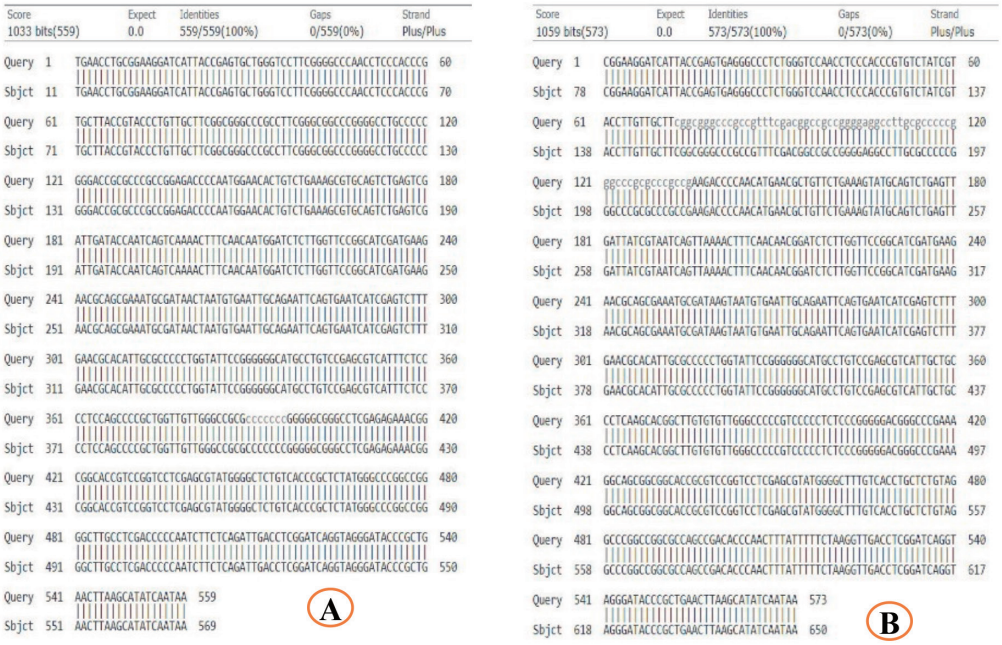

Fig. 5. Sequence of STCM1 (A). and Sequence STCM3 isolate (B).

forming stalks bearing spherical spores arranged in chains, with the spore stalks sunflower shaped (Fig. 3E). Initially, it was possible to identify the strains STCM1 and STCM3, which belong to *Aspergillus*.

The fungal–specific universal primer pairs ITS1 (forward) and ITS4 (reverse) effectively amplified the ITS region from DNA from all *Aspergillus* isolates. Capillary electrophoresis found sequence lengths ranging from 550 to 600 bp (Fig. 4). The morphological identification was corroborated by BLAST analysis of the ITS rDNA sequence data. The closest match (99 – 100 percent similarity) in the NCBI GenBank database was determined to be with distinct *Aspergillus* species. The results showed that the isolate STCM1 was 100% homologous to the ITS gene sequence of *Aspergillus aculeatus* (code: MN856264.1) (Fig. 5A), white STCM3 isolate was 100% homologous to the ITS gene sequence of *Aspergillus fumigatus* (Fig. 5B). (Code: MT597427.1).

The *Aspergillus aculeatus* was identified as a pathogen of grape berries in southwestern Ontario (Jarvis *et al.*, 1984). It is a wound pathogen that penetrates the berry via fractures induced by a partial detachment of fruits at the pedicel in tightly packed bunches, as well as splits and insect punctures. Other studies have reported the presence of *Botryodiplodia theobromae* and *Aspergillus aculeatus* – as pathogen causing soft rots of

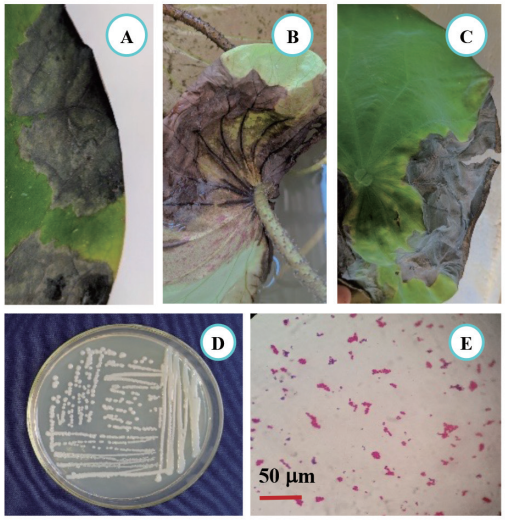

Fig. 6. Disease symptoms of Soft Rot and pathogen isolate STCV1
(A), (B), (C): Disease symptoms of Necrotic Brown Spot observed in lake;
(D): Colony morphology of STCV1 on LB, (E): Gram staining of STCV1.

Citrus fruits were grown on wheat offal medium (Adisa and Fojola, 1982).

Soft rot disease with typical symptoms includes soft rot, black color, necrosis, and water–soaked lesions at the edge of leaves and behind entire lotus leaves. We conducted isolates, and biochemical tests were performed to identify the pathogen from infected leaves. Strain STCV1 is a rod–shaped bacteria, non–flagellated, non–motile, and Gram–negative bacteria (Fig. 6E). Based on the morphological and biochemical test, the isolates were found to belong to Enterobacteriaceae.

After observing the colony morphology and microscopic visualizations, as shown in Fig. 6. STCV1 was further identified based on 16S rRNA sequence analysis. 27F–AGAGTTTGATCCTGGCTCAG was used as the forward primer, and the reverse primer was 1492R–GGTTACCTTGTTACGACTTT. Based on the 16 S rRNA sequence, bacterial isolates were classified into the genus *Klebsiella*. With comparative analysis of the 16 S rRNA gene, both morphological and biochemical, we identified the strain as *Klebsiella pneumoniae*, with 99.93% similarity.

Recently, *Klebsiella pneumoniae* is emerged as an important bacterial plant pathogen in Asia. The strain *Klebsiella pneumoniae* KpC4 was identified as a causative agent of bacterial top rot in maize, and has been observed in many areas of Yunnan province, China. In reports by Liu *et al.* (2015), it was reported to be a plant pathogen on onion bulbs causing internal tissue decay (soft rot) in Guangdong province, China. A previous report by Ajayasree and Borkar showed that *Klebsiella pneumoniae* causes root bark necrosis and wilt disease on pomegranate trees in India.

Antifungal and antibacterial activities of silver nanoparticles

The inhibitory effect of fungal mycelia growth was investigated in PDA medium containing different concentrations of 0.1, 1, 10, 20, and 30 mg/L (ppm) of silver nanoparticles (Fig. 7). The results were given in Fig. 7 and Fig. 8. There was a positive correlation between increased AgNPs concentration and antifungal efficacy. In addition, the size of the colonies decreased with the increased concentrations of silver nanoparticles. The results showed a very significant effect of synthesized silver nanoparticles on the mycelium growth of *Aspergillus* sp. More than 95% of the inhibitory effect on fungal growth was demonstrated on the *Aspergillus* sp. (96.72% with *Aspergillus aculeatus*, 97.22% with *Aspergillus fumigatus*) treated with AgNPs 30 mg/L. However, no significant differences were found among the control, 0.1, and 1 mg/L concentrations, with 0, 0.68, and 1.38% inhibition rates, respectively. In *Aspergillus fumigatus*, there were no significant differences when treated with 0.1 mg/L and 1 mg/L of silver nanoparticles with approximately 10% growth inhibitory (9.83%, 11,47%, respectively).

In general, the inhibition increased with the concentration of silver nanoparticles. These findings are in agreement with those obtained by Park *et al.* (2006); Kim *et al.* (2009); and Fatimah Al–Otibi (2021) reported

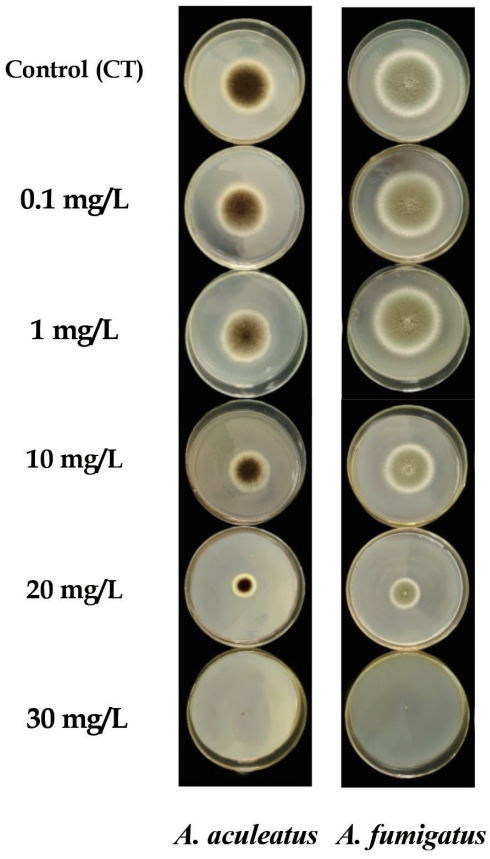

Fig. 7. Inhibition effect of silver nanoparticles (AgNPs) against fungal pathogen on PDA *in vitro*. Images were captured after culture plates had been incubated for 5 days at 28°C.

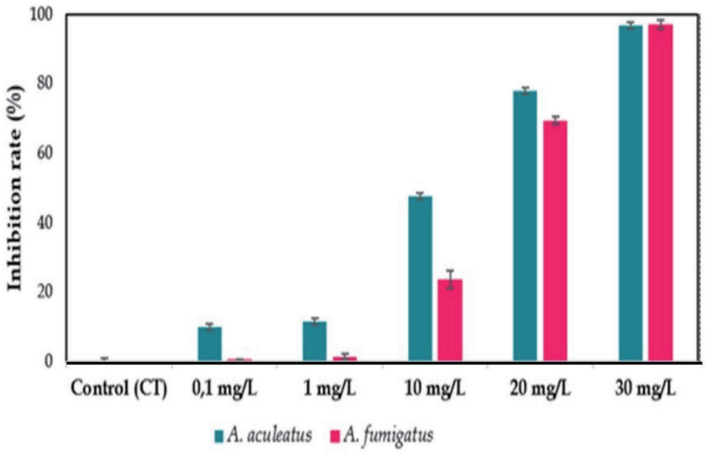

Fig. 8. Inhibition rate (%) of silver nanoparticles (AgNPs) against fungal pathogen.

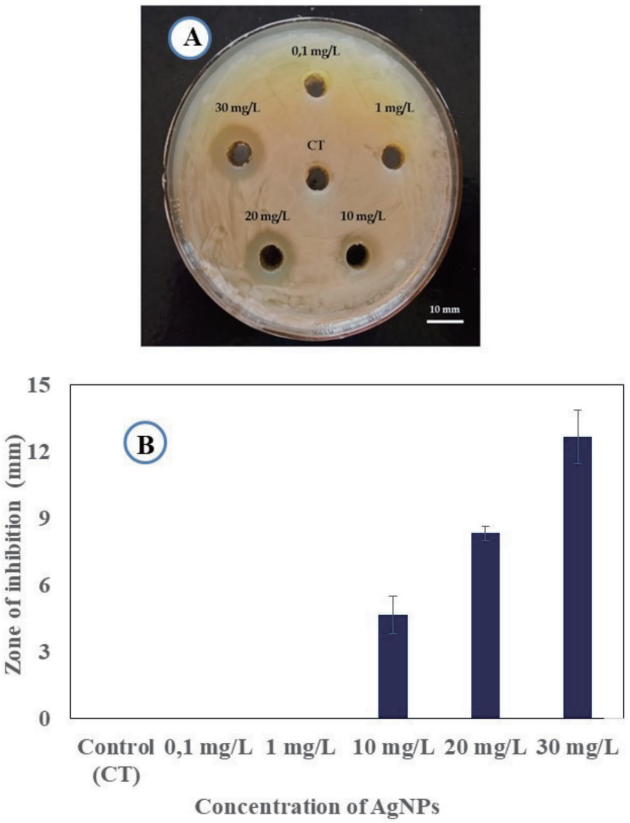

Fig. 9. Inhibition effect of silver nanoparticles (AgNPs) against bacterial pathogen.
(A). Zone of inhibition of silver nanoparticles; (B). bar graph showing zone of inhibition introduced by AgNPs against *Klebsiella pneumonia*. Images were captured after plates had been incubated for 24 hours at 35°C.

that Ag ions and silver nanoparticles had a significant effect on plant pathogenic fungi, *Bipolaris sorokiniana*, *Fusarium solani*, *Raffaelea* species, and Colletotrichum species.

In this study, we also conducted a detailed study on the role of concentration for the antibacterial activity of silver nanoparticles against *Klebsiella pneumoniae* – caused soft rot disease in *N. nucifera* (*cv*. concave white lotus). Fig. 9A, 9B shows the resulting zone of inhibition observed against *Klebsiella pneumoniae*. The larger inhibition zone was detected for treated with AgNPs at 10 mg/L, 20 mg/L, and 30 mg/L concentrations. No detected antibacterial "halo" with treated AgNPs at lower concentrations of 10 mg/L (0.1 mg/L, 1 mg/L)

Management of fungal and bacterial diseases on crops is economically essential. There have been numerous previous reports of silver nanoparticles' antimicrobial, antifungal use in treating *Escherichia coli*, *Staphylococcus aureus*, *Bacillus subtilis*, *Klebsiella mobilis*, *Mycobacterium tuberculosis*, and *Candida albicans*. This study confirms that silver nanoparticles have significant inhibitory effects on colony formation from conidia of *Aspergillus fumigatus*, *Aspergillus aculeatus*, and *Klebsiella pneumonia* – a pathogens–caused disease of a white lotus. The exact mechanisms of AgNPs against plant pathogens (bacteria, fungi) remain unknown. However, many studies have found that the electrostatic attraction between microorganisms; negatively charged cell membranes, such as bacteria, viruses, and fungus: and, positively charged nanoparticles play a critical role in the antibacterial activity of nanomaterials. Therefore, it was believed that silver nanoparticles with large surface areas could quickly form Ag+, binding to functional groups (–SH) of proteins and this resulted in protein denaturation. Besides, the antimicrobial activities of silver nanoparticles may result from a loss or inhibition of replication activity that inactivates the cellular proteins and enzymes of the pathogens (Feng QL, 2000).

The results have shown that silver nanoparticles can inhibit the growth and development of bacterial and fungal strains. Based on the findings of this study, silver nanoparticles are one of the most effective solutions for disease management on the white lotus (*Nelumbo nucifera*) *in vivo*. AgNPs green synthesis is considered less harmful, toxic, and cost–effective than other methods. This study promises the application of silver nanomaterials in the prevention and control of diseases on lotus plants caused by microbial agents, improving both the quality and quantity of white lotus.

CONCLUSION

This study has isolated and identified fungal and bacterial (*Aspergillus fumigatus*, *Aspergillus aculeatus*, *Klebsiella pneumoniae*) caused diseases in white lotus (*Nelumbo nucifera*). Endophytes can act as potential pathogens of white lotus, capable of inflicting severe damage to cultivate. Silver nanoparticles show significant antibacterial activity, antifungal against plant pathogens. Therefore, AgNPs could be a good alternative for development as an antibacterial, antifungal agent in this lotus variety. AgNPs can lead to valuable findings in various applications in agriculture, providing a novel and sustainable alternative in the food and agriculture sectors for disease management and control.

AUTHOR CONTRIBUTIONS

Nguyen Quang Hoang Vu contributed to the study conception, design, material and sample preparation, and analysis. The disease symptoms, isolation and identification of the fungal, bacterial pathogen of the manuscript was written by Hoang Tan Quang. Hoang Thi Kim Hong designed and supervised the research work. Sakae Agarie critically reviewed the manuscript with valuable suggestions comments. All authors read and approved the final manuscript.

ACKNOWLEDGEMENTS

Nguyen Quang Hoang Vu was funded by Vingroup Joint Stock Company and supported by the Domestic PhD Scholarship Programme of Vingroup Innovation Foundation (VINIF), Vingroup Big Data Institute (VINBIGDATA), code [VINIF.2021.TS.145].

REFERENCES

Adisa, V. A., and A. O. Fajola 1982 Pectinolytic enzymes associated with the soft rots of Citrus sinensis caused by *Aspergillus aculeatus* and *Botryodiplodia theobromae*. *Mycopathologia*, **77**(1): 47–50. https://doi.org/10.1007/BF00588657

Aguilar–Méndez, M. A., Martín–Martínez, E. S., Ortega–Arroyo, L., Cobián–Portillo, G., and E. Sánchez–Espíndola 2011 Synthesis and characterization of silver nanoparticles: Effect on phytopathogen *Colletotrichum gloesporioides*. *Journal of Nanoparticle Research*, **13**(6): 2525–2532. https://doi.org/10.1007/s11051–010–0145–6

Akpinar, I., Unal, M., and T. Sar 2021 Potential antifungal effects of silver nanoparticles (AgNPs) of different sizes against phytopathogenic *Fusarium oxysporum* f. sp. radicis–lycopersici (FORL) strains. *SN Applied Sciences*, **3**(4). https://doi.org/10.1007/s42452–021–04524–5

Aladame, N 1987 Bergey's manual of systematic bacteriology. *Annales de l'Institut Pasteur / Microbiologie*, **138**(1). https://doi.org/10.1016/0769–2609(87)90099–8

. Al–Otibi, F., Perveen, K., Al–Saif, N. A., Alharbi, R. I., Bokhari, N. A., Albasher, G., Al–Otaibi, R. M., and M. A. Al–Mosa 2021 Biosynthesis of silver nanoparticles using Malva parviflora and their antifungal activity. *Saudi Journal of Biological Sciences*, **28**(4): 2229–2235. https://doi.org/10.1016/j.sjbs.2021.01.012

An, C., Sun, C., Li, N., Huang, B., Jiang, J., Shen, Y., Wang, C., Zhao, X., Cui, B., Wang, C., Li, X., Zhan, S., Gao, F., Zeng, Z., Cui, H., and Y. Wang 2022 Nanomaterials and nanotechnology for the delivery of agrochemicals: strategies towards sustainable agriculture. In *Journal of Nanobiotechnology*, **20**(1): 11. https://doi.org/10.1186/s12951–021–01214–7

Ajayasree, T. S., S. G. Borkar 2018 Biochemical characteristics of plant pathogenic *Klebsiella pneumoniae* causing root bark necrosis and wilt in pomegranate. *Journal of Applied Biotechnology and Bioengineering*, **5**(4): 222–225 https://doi.org/10.15406/jabb.2018.05.00141

Bartlett, D. W., Clough, J. M., Godwin, J. R., Hall, A. A., Hamer, M., and B. Parr–Dobrzanski 2002 The strobilurin fungicides. In *Pest Management Science*, **58**: 649–62. https://doi.org/10.1002/ps.520

Chen, C. C., Chen, Y. Y., Yeh, C. C., Hsu, C. W., Yu, S. J., Hsu, C. H., Wei, T. C., Ho, S. N., Tsai, P. C., Song, Y. D., Yen, H. J., Chen, X. A., Young, J. J., Chuang, C. C., and H. Y. Dou 2021 Alginate–Capped Silver Nanoparticles as a Potent Anti–mycobacterial Agent Against *Mycobacterium tuberculosis*. *Frontiers in Pharmacology*, **12**: 746496. https://doi.org/10.3389/fphar.2021.746496

Feng, Q. L., Wu, J., Chen, G. Q., Cui, F. Z., Kim, T. N., and J. O. Kim 2000 A mechanistic study of the antibacterial effect of silver ions on *Escherichia coli* and *Staphylococcus aureus*. *Journal of Biomedical Materials Research*, **52**(4): 662–668. https://doi.org/10.1002/1097–4636(20001215)52:4<662::AID–JBM10>3.0.CO;2–3

Franci, G., Falanga, A., Galdiero, S., Palomba, L., Rai, M., Morelli, G., and M. Galdiero 2015 Silver nanoparticles as potential antibacterial agents. In *Molecules*, **20**(5): 8856–8874. https://doi.org/10.3390/molecules20058856

He, X., Deng, H., and H. M. Hwang 2019 The current application of nanotechnology in food and agriculture. In *Journal of Food and Drug Analysis*, **27**(1): 1–21. https://doi.org/10.1016/j.jfda.2018.12.002

Hong, H. T. K., Vu, N. Q. H., Hanh, N. T. N., Ha, T. T., and L. Q. T. Dung 2021 Study on the *In vitro* and *In vivo* Antifungal Activities of Nano–silver against *Mycoleptodiscus indicus* causing Leaf Blight on Lotus in Vietnam. *Indian Journal of Agricultural Research*. https://doi.org/10.18805/ijare.af–685

Jarvis, W. R 1984 Bunch Rot of Grapes Caused by *Aspergillus aculeatus*. *Plant Disease*, **68**(1): 718–719. https://doi.org/10.1094/pd–68–718

Kim, J. S., Kuk, E., Yu, K. N., Kim, J. H., Park, S. J., Lee, H. J., Kim, S. H., Park, Y. K., Park, Y. H., Hwang, C. Y., Kim, Y. K., Lee, Y. S., Jeong, D. H., and M. H. Cho 2007 Antimicrobial effects of silver nanoparticles. *Nanomedicine: Nanotechnology, Biology, and Medicine*, **3**(1): 95–101. https://doi.org/10.1016/j.nano.2006.12.001

Kim, S. W., Jung, J. H., Lamsal, K., Kim, Y. S., Min, J. S., and Y. S. Lee 2012 Antifungal effects of silver nanoparticles (AgNPs) against various plant pathogenic fungi. *Mycobiology*, **40**(1): 53–58. https://doi.org/10.5941/MYCO.2012.40.1.053

Kim, S. W., Kim, K. S., Lamsal, K., Kim, Y. J., Kim, S. bin, Jung, M., Sim, S. J., Kim, H. S., Chang, S. J., Kim, J. K., and Y. S. Lee 2009 An *in vitro* study of the antifungal effect of silver nanoparticles on oak wilt pathogen Raffaelea sp. *Journal of Microbiology and Biotechnology*, **19**(8): 760–764 https://doi.org/10.4014/jmb.0812.649

Kumar, S., Stecher, G., Li, M., Knyaz, C., and K. Tamura 2018 MEGA X: Molecular evolutionary genetics analysis across computing platforms. *Molecular Biology and Evolution*, **35**(6): 1547–1549. https://doi.org/10.1093/molbev/msy096

Liu, S., Lv, M., Gu, Y., and J. Zhou 2015 First report of bulb disease of onion caused by Subramanian, *of Science and Research (IJSR)*, **14**(7)

Pulimi, M., and S. Subramanian 2016 *Nanomaterials for Soil Fertilisation and Contaminant Removal*. In: Ranjan, S., Dasgupta, N., Lichtfouse, E. (eds) Nanoscience in Food and Agriculture 1. Sustainable Agriculture Reviews, Vol.20, Springer, Cham, pp: 229–246. https://doi.org/10.1007/978–3–319–39303–2_8

Rajwade, J. M., Chikte, R. G., and K. M. Paknikar 2020

Nanomaterials: new weapons in a crusade against phytopathogens. In *Applied Microbiology and Biotechnology*, **104**(4): 1437–1461. https://doi.org/10.1007/s00253–019–10334–y

Sadeghi, B., Jamali, M., Kia, S., Amini, a, and S. Ghafari 2010 Synthesis and characterization of silver nanoparticles for antibacterial activity. *Scanning Electron Microscopy*, **1**(2): 119–124 https://www.sid.ir/en/journal/ViewPaper.aspx?id=194433

Zhu, F 2017 Food Hydrocolloids Structures, properties, and applications of lotus starches. *Food Hydrocolloids*, **63**, 332–348 https://doi.org/10.1016/j.foodhyd.2016.08.034

Hue University Journal of Science: Agriculture and Rural Development
pISSN: 2588-1191; eISSN: 2615-9708
Vol. 132, No. 3C, 2023, P. 51–67, DOI: 10.26459/hueunijard.v132i3C.7275

Neofusicoccum parvum: A NOVEL PATHOGEN SPECIES CAUSING WILTED LEAF AND DIEBACK PETIOLES ON LOTUS (*Nelumbo nucifera*) IN THUA THIEN HUE, VIETNAM

Vu Quang Hoang Nguyen[1], Tram Thi Ngoc Tran[1], Lan Thuy Tran[1], Thi Thi Diem Pham[1], Quang Tan Hoang[1], Hong Thi Kim Hoang[2, 3]*

[1] Institute of Biotechnology, Hue University, Road No. 10, Phu Vang, Thua Thien Hue, Vietnam
[2] Biotechnology Department, College of Medicine and Pharmacy, Duy Tan University, Hoang Minh Thao St., Hoa Khanh Nam, Lien Chieu, Da Nang, Vietnam
[3] Institute for Research and Training in Medicine, Biology and Pharmacy, Duy Tan University, 254 Nguyen Van Linh St., Thanh Khe, Danang, Vietnam

* Correspondence to Hong Thi Kim Hoang <hoangtkimhong@duytan.edu.vn>
(*Received: August 7, 2023; Accepted: October 3, 2023*)

Abstract. Lotus (*Nelumbo nucifera*) is an essential species in many countries. In Vietnam, the lotus is a plant with cultural and spiritual significance, representing purity, spiritual growth, and enlightenment. However, petiole dieback and wilted dry leaves are severe diseases that weaken the host and decrease leaf photosynthesis, reducing lotus production. In this study, a new dieback and wilted leaf pathogen were identified via its morphology, phylogeny, and pathogenicity. Four representative Botryosphaeriaceae isolates from lotus fields in Hue, Phong Dien, and Phu Loc were selected for identification and pathogenicity testing. Based on morphological and phylogenetic analyses and by using the ribosomal internal transcribed spacer region (ITS) and β-tubulin (tub-2) gene sequences, we identified four isolates as *Neofusicoccum parvum*. In the pathogenicity test, typical symptoms appear on the inoculated lotus petioles, including dieback, curving, and wilted leaves. These symptoms are consistent with those observed in the field. In addition to identifying the pathogen species responsible for lotus disease, this study provides valuable insights into the taxonomy and phylogenetic relationships of new fungal pathogens that affect lotus fields. These findings can contribute to effective management strategies to control these diseases and improve lotus production. To the best of our knowledge, this is the first report of characterization and phylogenetic analysis of *N. fusicoccum* as the causal agent of wilted leaves and dieback disease in Thua Thien Hue, Vietnam.

Keywords: *Neofusicoccum parvum*, dieback disease, phylogeny, lotus, Vietnam

1 Introduction

The Botryosphaeriaceae are diverse fungi, including 24 genera of ecologically diverse host plants that are either plant pathogens, endophytes, or saprobes [1, 2]. The diseases associated with this family of fungi are often triggered by stressors, such as environmental stressors like drought, extreme temperature changes, heavy metals, nutrient deficiencies, and leaf injuries. These factors

can promote the pathogenicity of Botryosphaeriaceae species [2, 3]. However, they can also be primary pathogens, especially when non-adapted hosts are exposed to an exotic pathogen [4–7]. In recent years, there have been a growing number of reports on diseases caused by *Neofusicoccum* species in numerous countries. For example, *Neofusicoccum parvum* has been identified as a pathogen in different plants, including *Zanthoxylum bungeanum*, *Rhododendron*, *Eucalyptus* spp. in China [8] and nut rot of chestnut (*Castanea sativa*). In the United States, *N. parvum* has been identified as the cause of dieback and canker of hemp (*Cannabis sativa*) in Italy, causing brown spots on gallnuts of *Rhus potaninii* in China, black spots of *Rosa chinensis* in China [9], twig blight and branch dieback of walnut in Turkey [10], stem canker and dieback in blueberries in Chile [11], and wilting and stem rot of *Santalum album* in China [9]. It is worth noting that *N. luteum*, *N. batangarum*, *N. mangiferae*, and some other species in *Neofusicoccum* have also been reported to be related to various plant diseases. It is important to mention that in the past, several species of *Neofusicoccum* were incorrectly classified because of their morphological similarities. However, with the development of phylogenetic analysis, most new species have been discovered, and some known species have been reclassified. Therefore, the identification and management of *Neofusicoccum* species have become increasingly important in the field of plant pathology.

Lotus (*Nelumbo nucifera* Gaertn.) is a perennial aquatic crop that is grown and consumed in Asia for food, ornamental, and medicinal purposes. Currently, despite the importance attributed to the species of this family, knowledge of the taxonomy and diversity of *Neofusicoccum* pathogens associated with the lotus in Vietnam is limited. During the summer of 2022–2023, petioles blight and dieback symptoms were observed in several lotus fields in Thua Thien Hue, Central Vietnam. The present study aims to identify *Neofusicoccum* isolates collected from lotus with symptoms of dieback, blight, and wilted leaves. Species were identified based on their morphology and comparison of the DNA sequence data for ITS rDNA and β-tubulin (tub-2). The taxonomy and phylogenetic relationships of pathogen isolates were investigated, and their pathogenic abilities were determined.

2 Materials and methods

Sampling, isolation, and purification of pathogenic fungi

From 2022 to 2023, nine samples were collected from lotus fields in three regions in Thua Thien Hue, Vietnam (Hue, Phong Dien, and Phu Loc). Before being transferred to the laboratory for further testing, the samples were placed in plastic bags labelled with the date, site, and symptoms. Infected tissues were cut into small pieces (5 × 5 mm), and their surfaces were disinfected with 1% sodium hypochlorite (NaOCl) for 30 seconds and washed three times with sterile distilled water. Tissue samples were dried on sterile absorbent paper and transferred onto WA (water

agar) plates. The inoculated plates were incubated at 30 °C for seven days. To obtain pure culture, we transferred fungal hyphae to fresh potato dextrose agar (PDA) plates for further culture. Obtained isolates were preserved in 50% (v/v) glycerol at −40 °C for future use.

Table 1. List of nine isolates collected from *N. nucifera* in Thua Thien Hue province in this study

Isolate Code	Source – Host plant	Collection date	Geographical Origin
HX.DB.SH.01	*N. nucifera* cv. Cao san pink/ Petiole	June, 2022	Dong Ba, Hue City, Thua Thien Hue province 16°28'40.6"N 107°35'01.7"E
HX.DB.SH.02	*N. nucifera* cv. Cao san pink/ Petiole	July, 2022	Thuan Hoa, Hue City, Thua Thien Hue province 16°28'07.4"N 107°34'19.3"E
HX.DB.SH.03	***N. nucifera* cv. Cao san pink/ Petiole**	March, 2023	Dong Ba, Hue City, Thua Thien Hue province 16°28'40.1"N 107°35'02.4"E
HX.DB.SH.04	***N. nucifera* cv. white/ Leaf**	March, 2023	Dong Ba, Hue City, Thua Thien Hue province 16°28'38.4"N 107°35'03.3"E
HX.DB.SH.05	*N. nucifera* cv. white/ Petiole	May, 2023	Dong Ba, Hue City, Thua Thien Hue province 16°28'40.4"N 107°35'02.0"E
KN.SH.PD.1004	***N. nucifera* cv. Cao san pink/ Leaf**	April, 2022	Phong Hien, Phong Dien District, Thua Thien Hue province 16°33'26.1"N 107°27'17.6"E
KN.PH.PD.1004	*N. nucifera* cv. Cao san pink/ Leaf	May, 2023	Phong Hien, Phong Dien District, Thua Thien Hue province 16°33'21.9"N 107°27'22.8"E
TN.TL.SH.02	*N. nucifera* cv. white/leaf	April, 2023	Phu Loc District, Thua Thien Hue province 16°16'26.3"N 107°52'09.7"E
TN.TL.SH.03	***N. nucifera* cv. white/Petiole**	April, 2023	Phu Loc District, Thua Thien Hue province 16°16'21.3"N 107°52'28.5"E

Morphological analysis

The isolates were cultured on PDA to observe colony and conidia morphology. Mycelial discs of 5 × 5 mm diameters were inoculated at the centre of PDA plates and incubated in the dark at ambient temperature (30 ± 2 °C). Colony diameters were measured after seven days, and cultural features were examined and photographed. The characteristics of conidia were observed under an Olympus BX51 photographic microscope.

DNA extraction, PCR amplification

Pathogenic fungi were inoculated and grown for seven days on PDA; then, the mycelia were collected and harvested by using Whatman filter paper. Fungal DNA genomic was extracted by using the Genomic DNA Extraction Kit, following the manufacturer's instructions (ABT, Vietnam). Polymerase chain reaction (PCR) amplification of the ribosomal DNA internal transcribed spacer (ITS) region, β-tubulin (tub-2) region, was performed using the primers pairs ITS1/ITS4, and βt2a/Bt-2b [12, 13]. ITS1 (5'-TCCGTAGGTGAACCTGCGG-3')/ITS4 (5'-TCCTCCGCTTATTGATATGC-3'); βt2a (5'-GGTAACCAAATCGGTGCTGCTTTC-3')/ βt2b (5' ACCCTCAGTGTAGTGACCCTTGGC-3'). Polymerase chain reaction amplification was carried out in a SimpliAmp™ Thermal Cycler (Applied Biosystems, Thermo Fisher Scientific Inc., USA) in a 50 µL reaction mixture containing 25 µL of Go Taq Green 2X Master Mix (Promega, USA), 5 µL (50 ng) of the DNA template, 5 µL of each primer (10 pmol), and 15 µL of ddH_2O.

The PCR conditions were as follows: initial denaturation at 95 °C for five minutes, followed by 35 cycles: 95 °C for 30 seconds, annealing at a suitable temperature for 30 seconds, and 72 °C for 60 seconds. The final extension was performed at 72 °C for seven minutes. The annealing temperature for each gene was 52 °C for ITS and 55 °C for tub-2.

Sequencing and phylogenetic analysis

Polymerase chain reaction products were sequenced at the First BASE sequencing service in Malaysia. The sequences obtained were read and compared by using The Basic Local Alignment Search Tool (BLASTn) in GenBank at National Center for Biotechnology Information NCBI ((http://www.ncbi.nlm.nih.gov, accessed on 15 July 2023) (Table 2).

The DNA sequences obtained from both strands were assembled to obtain consensus sequences for each isolate by using BioEdit v7.0.5 [14]. Multiple sequence alignment was manually performed with the closely related reference sequences available in the NCBI database by using MUSCLE in MEGA 11 software under default parameters. Aligned gene regions were adjusted manually where necessary. Concatenated alignment was performed by using MEGA 11 software [15]. To establish the identity of fungal isolates, we conducted phylogenetic analysis by

using a concatenated session formed by two loci (ITS, tub-2). The phylogenetic tree was reconstructed according to the maximum likelihood method by using IQ-TREE v. 2.1.3 [16]. The ModelFinder was used to determine the best-fit model [17]. Branch support was determined by using 10,000 ultra-bootstraps, a Bayesian posterior probabilities support, and 10,000 SH-aLRT bootstrap replicates. The resulting trees were plotted by using FigTree v. 1.4.2 (http://tree.bio.ed.ac.uk/software/figtree), Interactive Tree of Life (iTOL) v.6 [18], and edited by using PowerPoint (Microsoft, CA, USA) and Adobe Illustrator CC 2021 (Adobe Systems, CA, USA).

Pathogenicity tests

The pathogenicity and virulence of four representative isolates of *N. parvum* were examined via Koch's postulates. Lotus plants (*N. nucifera* cv. Cao san – high yield pink, and cv. white) at the two- to three-leaf stage were used for all inoculation tests in this study. The inoculation points of petioles were surface-disinfected with 1% sodium hypochlorite solution for 1 min, followed by 70% ethanol for 2 min with filter paper. Mycelium plugs (6 × 6 mm) of ½ PDA were cut from an actively growing colony, placed on inoculation points, and wrapped in paraffin. The plants were kept under high humidity conditions (>85% relative humidity) in a covered plastic container for 1–3 days at 28 °C. Plants were then transferred to a net house maintained at ambient temperature (30 ± 2 °C under a 12 h/12 h photoperiod). The area of the lesion developed on the inoculated petioles was measured with a grid table, converted with ImageJ v1.5.2 (National Institute of Health, USA). For each trial, we used three plant replicates (three inoculation points/plant) for fungal inoculation. In the control plants, the sterile PDA plug was used for inoculation (control). Differences in lesion area were evaluated by using the one-way method ANOVA, and means were compared with Tukey's post-hoc test ($p < 0.05$) by using IBM SPSS Statistics v.20 software. To confirm Koch's postulates, the fungal pathogens from symptomatic inoculated leaves and petioles were reisolated and reidentified by using morphological characteristics.

3 Results

Fungal isolation and morphological identification

The symptomatic lotus plants in the field exhibit different symptoms, characterized with severely infected petiole browning and leaf browning and wilting (Fig. 1b, 1c, and 1d). The tissues with symptoms were collected for fungal pathogen isolation. Nine isolates of pathogens were successfully recovered from the diseased samples collected from the lotus fields in the study location. These isolates were fast-growing on PDA and formed abundant aerial mycelia that were initially white, turning grey to dark grey over time (after 4–5 days). The reverse of the colonies

was white, which also became greyish to greenish-grey with ageing (14–15 days). These morphological characteristics are similar to those of other members of the parvum-ribis species complex. The colonies formed dark pycnidia in pine needles (Figure 2e). The conidial sizes range from 17.5–21.3 (avg. 19.8) µm × 9.7–12.2 (10.5) µm.

Fig. 1. Disease symptoms observed on *N. nucifera* from lotus fields in Dong Ba, Hue City, Thua Thien Hue

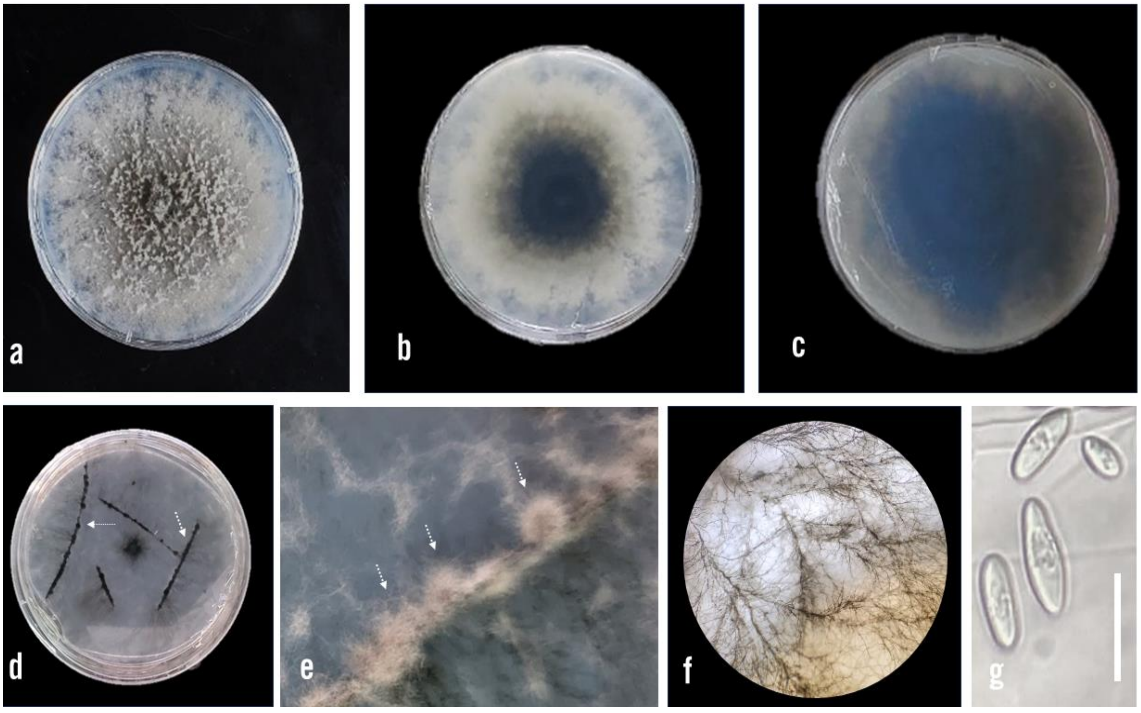

Fig. 2. *Neofusicoccum parvum* (HX.DB.SH.03). a: Upper side of colony grown on PDA (five days); b: Reverse side; c: Aged colony on PDA (14 days); d: Conidiomata on WA 2% + pine needles; e: Pycnidia and conidia induced to form after 15 days in WA 2% + pine needles; f: Hyphae form in WA 2% + pine needles; g: Conidia. Scale bar = 20 μm.

Molecular identification and phylogenetic analysis

The representative isolates: HX.DB.SH.03 (isolated from cultivar Cao san/petiole), HX.DB.SH.04 (cv. white/leaf), KN.SH.PD.1004 (cv. Cao san/leaf), and TN.TL.SH.03 (cv. white/petiole) were selected for molecular identification and phylogenetic analysis. The amplicon size of these isolates is 500–650 bp for ITS and 300–400 bp for tub-2. The BLASTn analysis homology of the sequences indicates that the sequences from the present study match well with the reliable reference sequences of *N. parvum* and show 100% sequence similarity in ITS with BRIP66334, CMW28386, 99.78% in tub-2 with L12, KARE1198.

Table 2. Taxa of isolates and their GenBank accession numbers used in the phylogenetic analysis

Species	Accession Number	ITS	TUB-2	Host	Origin	
N. arbuti	CBS116131	AY819720	KF531793	*Arbutus menziesii*	USA	**Type**
N. australe	CMW6837 = CBS139662	AY339262	AY339254	*Acacia sp.*	Australia	
N. batangarum	**CBS124924 = CMW28363**	FJ900607	FJ900634	*Terminalia catappa*	Cameroon	**Type**
N. batangarum	CBS124923 = CMW28320	FJ900608	FJ900635	*Terminalia catappa*	Cameroon	
N. brasiliense	**CMM1338**	JX513630	KC794031	*Mangifera indica*	Brazil	**Type**
N. brasiliense	CMM1285	JX513628	KC794030	*Mangifera indica*	Brazil	
N. cordaticola	**CBS123634**	EU821898	EU821838	*Syzygium cordatum*	South Africa	**Type**
N. cordaticola	CBS123635	EU821903	EU821843	*Syzygium cordatum*	South Africa	
N. cryptoaustrale	**CBS 122813 = CMW23785**	FJ752742	FJ752756	*Eucalyptus sp.*	South Africa	**Type**
N. eucalypticola	**CBS115679 = CMW6539**	AY615141	AY615125	*Eucalyptus grandis*	Australia	**Type**
N. eucalypticola	CBS115766 = CMW6217	AY615143	AY615127	*Eucalyptus rossi*	Australia	
N. eucalyptorum	**CBS115791 = CMW10125**	AF283686	AY236920	*Eucalyptus grandis*	South Africa	**Type**
N. hellenicum	**CERC1947**	KP217053	KP217069	*Pistacia vera*	Greece	**Type**
N. hellenicum	CERC1948	KP217054	KP217070	*Pistacia vera*	Greece	
N. hongkongense	CERC2973	KX278052	KX278261			
N. hongkongense	CERC2967	KX278050	KX278259			
N. kwambonambiense	CBS123641 = CMW14140	EU821919	EU821859	*Syzygium cordatum*	South Africa	
N. kwambonambiense	**CBS 123639 = CMW14023**	MH863317	EU821840	*Syzygium cordatum*	South Africa	**Type**
N. luteum	**CBS110299**	AY259091	DQ458848	*Vitis vinifera*	Portugal	**Type**
N. luteum	CBS110497	EU673311	EU673092	*Vitis vinifera*	Portugal	
N. lumnitzerae	**CMW 41469**	KP860881	KP860801	*Luminitzera racemosa*	South Africa	**Type**

Species	Accession Number	ITS	TUB-2	Host	Origin	
N. macroclavatum	**CBS118223**	DQ093196	DQ093206	*Eucalyptus globulus*	Australia	**Type**
N. mediterraneum	PD82	GU251192	GU251852	*almond*	USA	
N. mediterraneum	**CBS121718**	GU251176	GU251836	*Eucalyptus sp.*	Greece	**Type**
N. nonquaesitum	**CBS126655 = PD484**	GU251163	GU251823	*Umbellularia californica*	USA	**Type**
N. occulatum	**CBS 128008 = MUCC227**	EU301030	EU339472	*Eucalyptus grandis*	Australia	**Type**
N. occulatum	MUCC 286	EU736947	EU339474	*Eucalyptus pellita*		
N. parvum	CPC31234	MN860181	MN905746	*Persea americana*	Greece	
N. parvum	CERC 3503	KX278059	KX278268	*E. urophylla × E. grandis*	China	
N. parvum	MAN55	KY052933	KY000117			
N. parvum	MFLUCC 11-0184	JX646795	JX646843			
N. parvum	**CBS 138823 = ATCC58191 = CMW9081**	AY236943	AY236917	*Populus nigra*	New Zealand	**Type**
N. parvum	LC013	OM392021	OM453641	*Macadamia*	China	
N. pennatisporum	**MUCC510**	EF591925	EF591959	*Allocasuarina fraseriana*	Australia	**Type**
N. ribis	**CBS 115475**	AY236935	AY236906			**Type**
N. stellenboschiana	**CBS110864 = CPC4598**	AY343407	KX465047	*Vitis vinifera*	South Africa	**Type**
N. stellenboschiana	CPC 31232	MN860179	MN905744	*Persea americana*	Greece	
N. umdonicola	**CBS 123645 = CMW14058**	EU821904	EU821844	*Syzygium cordatum*	South Africa	**Type**
N. umdonicola	CBS 123646 = CMW14060	EU821905	EU821845	*Syzygium cordatum*	South Africa	
N. vitifusiforme	**CBS110887 = STE-U 5050**	AY343382	KX465061	*Vitis vinifera*	South Africa	**Type**
Botryosphaeria dothidea	**CBS 115476**	AY236949	AY236927			**Type**

Strains bolded are ex-type or ex-epitype. ATCC: *American Type Culture Collection, Virginia, USA*; CBS: *Culture collection of the Westerdijk Fungal Biodiversity Institute, Utrecht, The Netherlands*; CMM: *Culture Collection of*

Phytopathogenic Fungi Prof. Maria Menezes, Federal Rural University of Pernambuco, Brazil; CMW: *Culture Collection of the Forestry and Agricultural Biotechnology Institute (FABI), University of Pretoria, Pretoria, South Africa*; CPC: *Culture collection of Pedro Crous, housed at CBS*; CERC: *China Eucalypt Research Center, Chinese*; MFLUCC: *Mae Fah Luang University Culture Collection, Thailand*; ICMP: *International Collection of Micro-organisms from Plants, Landcare Research, New Zealand*.

To further identify these isolates, we performed the phylogenetic analysis with ITS and tub-2 sequence alignment comprising 45 isolates with *Boytryosphaeria dothidea* CBS115476 as the outgroup for individual loci sequenced as well as on the combined dataset (Fig. 3). The best-fit models of nucleotide substitution used in the analysis of individual genes were as follows: TNe + I + G4 (ITS) and HKY + F + G4 (tub-2). The tree topologies resulting from ML analysis of independent alignments of ITS, a portion of the tub-2 gene, and a concatenated data set containing both loci were congruent, with strongly supported species-level clades for *N. parvum*. The tree constructed with optimal log-likelihood of ML analysis is –2681.773. The HKY+F+I+G4 best-fit model was chosen according to the Bayesian information criterion (BIC). The estimated base frequencies were recorded as follows: *A* = 0.209; *C* = 0.321; *G* = 0.249; *T* = 0.20; while substitution rates were established as *AC* = 1; *AG* = 8.83977; *AT* = 1; *CG* = 1; *CT* = 8.83977; *GT* = 1; the gamma distribution shape parameter (α) is 0.611. The results show that the four isolates: HX.DB.SH.03, HX.DB.SH.04, KN.SH.PD.1004, and TN.TL.SH.03 cluster with strong statistical support in the clade contain the type strain *N. parvum* CMW9081 (SH-aLRT/PP/MLBS: 97.4/1/98-ITS, 92.1/1/94-tub2, 96.7/1/99-concatenated ITS+tub), where *N. batagarum*, *N. umdonicola*, and *N. ribis* are associated (PP/MLBS = 1/93) as the closest sister species of these pathogenic fungi.

The phylogenetic relationships of the *Neofusicoccum* species fully match the topology of the phylogeny tree reported by Bezerra et al., Hilário et al., and Lopes et al. [19–21]. The combined sequence data of these isolates group with the high bootstrap value of the reference *N. parvum* CMW9081 (Fig. 3). Therefore, these isolates were confirmed as *N. parvum* based on molecular identification.

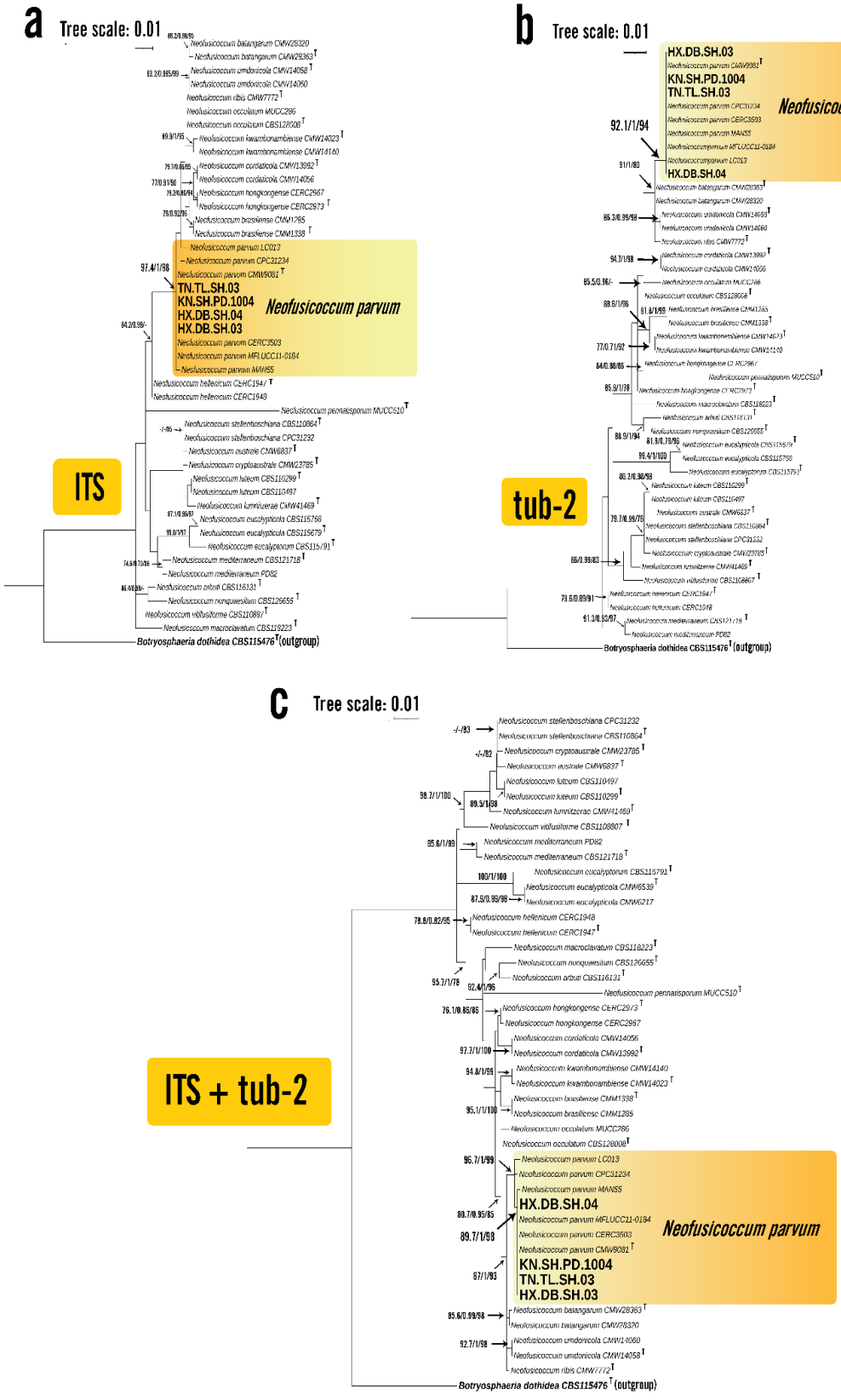
a
Tree scale: 0.01
ITS
Neofusicoccum parvum
TN.TL.SH.03
KN.SH.PD.1004
HX.DB.SH.04
HX.DB.SH.03
Botryosphaeria dothidea CBS115476 (outgroup)
b
Tree scale: 0.01
tub-2
Neofusicoccum parvum
HX.DB.SH.03
KN.SH.PD.1004
TN.TL.SH.03
HX.DB.SH.04
Botryosphaeria dothidea CBS115476 (outgroup)
c
Tree scale: 0.01
ITS + tub-2
Neofusicoccum parvum
HX.DB.SH.04
KN.SH.PD.1004
TN.TL.SH.03
HX.DB.SH.03
Botryosphaeria dothidea CBS115476 (outgroup)

Fig. 3. Phylogenetic trees based on maximum likelihood (ML) analysis for species in *Neofusicoccum* sp. a. ITS region; b. tub-2 gene region; c. combination of ITS + tub regions. Isolates sequenced in this study are in bold. Bootstrap support values are shown at each node (SH-aLRT/BPP/MLBS). Isolates representing type sequences are marked with 'T'. *Botryosphaeria dothidea* CBS 115476 was used as the outgroup taxon. The bar indicates the substitutions number per position.

N. parvum has previously been reported to cause canker and dieback symptoms in blueberries in Chile, avocado orchards and *Eucalyptus* in Spain [22], walnut in Turkey [23], grapevine trunk in Algeria [24], *Cannabis sativa* in Italy, and Canada [25, 26], *Olea europaea* in Italy [27], sequoias (*Sequoiadendron giganteum*) in Switzerland [4], and *Osmanthus fragans* in China [28]. It was reported causing stem end rot in mango, leaf spot disease of *Machilus thunbergii* – Japan, *Geodorum eulophioides*, *Cinnamomum cassia* in China [29, 30], and leaf blight of Indian hawthorn (*Rhaphiolepsis indica*) in Italy. To our best knowledge, this is the first report of *N. parvum* as a new agent associated with leaf spot and petioles dieback in *Nelumbo nucifera* in Vietnam. Furthermore, the lotus plants facing environmental stress or mechanical injuries due to natural disasters, such as strong winds, floods, and droughts, create favourable conditions, highly vulnerable to this pathogen. In addition, several studies have shown that fungi belonging to the Botryosphaeriaceae family can infiltrate plants via endophytic colonization, wounds, contaminated soil, and insect attacks [30, 31].

Pathogenicity tests

Morphological observations on microscopes show that all pathogen isolates are identical, and four isolates were selected for the pathogenicity tests. Fulfilling Koch's postulates shows that *Neofusicoccum* spp. are pathogens causing wilted leaves and dieback petioles on the lotus, the symptoms similar to those observed in the field.

The petioles inoculated with these isolates were inspected for the appearance of canker symptoms at the early stage (7–10 days post-inoculation (dpi)). All isolates cause lesions on the petioles, with larger lesion sizes observed with the wounded method. When the petioles were inoculated with the unwounded method, the disease area was smaller. As the disease progresses, the lesions expand longitudinally from the inoculation sites and spread to leaves, causing the leaves to turn brown, gradually curling and wilting. After 35–40 days, the plant-inoculated pathogen isolates completely dried and died. A cross-section of the fungal inoculated plant shows the rooting area of the internal xylem of petioles, and the diseased area has a dark brown colour. In contrast, the plants treated with sterile PDA (control) do not exhibit any signs of dieback (Fig. 4g).

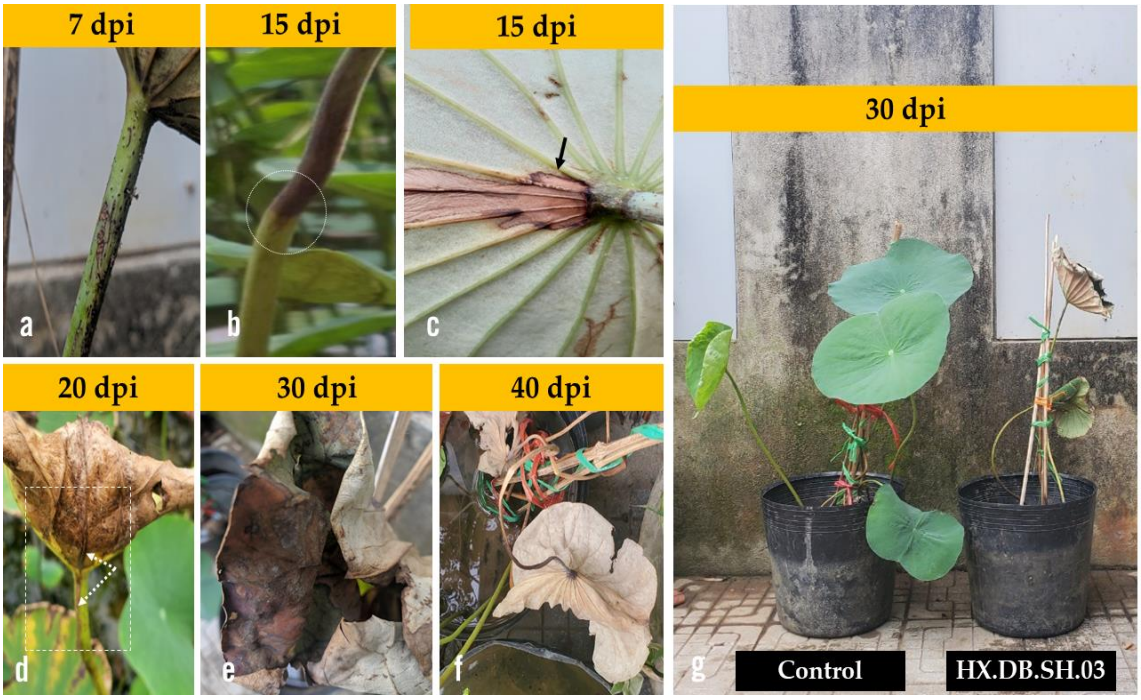

Fig. 4. Pathogenicity test results. Disease symptoms in different parts of lotus plant induced by *N. parvum* – isolate HX.DB.SH.03. a. Early stage (7dpi) with browning of necrotic areas; b, c. Lesion spread on petioles and leaves; d: e, f: leaves gradually curving, dry, and dead; g: The lotus plant-inoculated isolate HX.DB.SH.03 exhibited disease, while the control remained symptomless.

Since *Neofusicoccum* is known to have a wide host range, we investigated whether the isolates in this study could cross-infect a range of lotus cultivars (cv. white and cv. Cao san). Although all isolates cause dieback in both lotus cultivars, the area and speed of dieback development differ significantly, suggesting that virulence varies among isolates and inoculation methods. In the wounded method, there are significant differences in lesion areas produced on the *N. nucifera* inoculated petioles that range from 67.38 to 82.6 mm^2 for cv. Cao san lotus and 26.86–46.60 mm^2 for cv. white lotus. These findings suggest that *N. nucifera* cv. cao san is more susceptible to *N. parvum* infection than *N. nucifera* cv. white, with greater disease severity ($p < 0.05$).

Table 3. Area (mm^2) of lesion caused by four isolates *N. parvum* on petioles of various cultivar of lotus at 15 dpi

Inoculation method	Cultivar	HX.DB.SH.03	HX.DB.SH.04	KN.SH.PD.1004	TN.TL.SH.03
Agar plugs on wounded	cv. Cao san lotus	82.60 ± 5.32[a]	80.94 ± 5.11[a]	67.38 ± 2.31[b]	72.36 ± 4.54[b]
	cv.white lotus	45.06 ± 3.56[a]	46.60 ± 1.21[a]	26.86 ± 2.48[b]	30.18 ± 1.91[b]
	Control	0	0	0	0
Agar plugs on unwounded	cv. Cao san lotus	36.74 ± 1.06[a]	35.76 ± 2.25[a]	30.38 ± 1.99[b]	31.94 ± 2.24[b]
	cv.white lotus	25.92 ± 2.04[a]	26.74 ± 1.98[a]	20.66 ± 2.83[b]	21.02 ± 2.00[b]
	Control	0	0	0	0

Note: Average lesion area (mm^2) ± SD (standard deviation). The letters indicate that the treatments are significantly different ($p < 0.05$, Turkey HSD test). Data were recorded at 15 days post-inoculation (dpi).

4 Conclusion

In this study, we first reported *Neofusicoccum parvum* as a causal pathogen of petioles dieback, leaf blight, and curving lotus leaves in Thua Thien Hue, Vietnam. The pathogen was identified by using morphological features, multigene DNA sequencing, phylogenetic analysis, and pathogenicity testing. This information is useful in establishing quarantine measures and developing targeted disease management strategies.

Acknowledgements

This work was supported by a grant from Hue University (Grant number code: DHH2023-15-20). Nguyen Quang Hoang Vu was funded by Vingroup Joint Stock Company and supported by the Domestic Ph.D. Scholarship Programme of Vingroup Innovation Foundation (VINIF), Vingroup Big Data Institute (VINBIGDATA), code: [VINIF.TS.2020.TS.89; VINIF.2021.TS.145; VINIF.2022.TS.147].

References

1. Phillips, A. J. L., Alves, A., Abdollahzadeh, J., Slippers, B., Wingfield, M. J., Groenewald, J. Z. & Crous, P. W. (2013), The Botryosphaeriaceae: Genera and species known from culture, *Studies in Mycology*, 76. https://doi.org/10.3114/sim0021.
2. Slippers, B., Crous, P. W., Jami, F., Groenewald, J. Z. & Wingfield, M. J. (2017), Diversity in the Botryosphaeriales: Looking back, looking forward, *Fungal Biology*, 121(4). https://doi.org/10.1016/j.funbio.2017.02.002.
3. Mehl, J., Wingfield, M. J., Roux, J. & Slippers, B. (2017), Invasive everywhere? Phylogeographic analysis of the globally distributed tree pathogen lasiodiplodia theobromae, *Forests*, 8(5). https://doi.org/10.3390/f8050145.
4. Haenzi, M., Cochard, B., Chablais, R., Crovadore, J. & Lefort, F. (2021), Neofusicoccum parvum, a new agent of sequoia canker and dieback identified in Geneva, Switzerland, *Forests*, 12(4). https://doi.org/10.3390/f12040434.
5. Diniz, I., Batista, D., Pena, A. R., Rodrigues, A. S. B., Reis, P., Balde, A., Indjai, B., Catarino, L. & Monteiro, F. (2021), First report of dieback caused by Neofusicoccum batangarum in Cashew in Guinea-Bissau, In *Plant Disease*, 105(4). https://doi.org/10.1094/PDIS-10-20-2308-PDN.
6. Belair, M., Grau, A. L., Chong, J., Tian, X., Luo, J., Guan, X. & Pensec, F. (2022), Pathogenicity Factors of Botryosphaeriaceae Associated with Grapevine Trunk Diseases: New Developments on Their Action on Grapevine Defense Responses, *Pathogens*, 11(8). https://doi.org/10.3390/pathogens11080951.
7. Dissanayake, A. J., Phillips, A. J. L., Li, X. H. & Hyde, K. D. (2016), Botryosphaeriaceae: Current status of genera and species, *Mycosphere*, 7(7). https://doi.org/10.5943/mycosphere/si/1b/13.
8. Li, G. Q., Liu, F. F., Li, J. Q., Liu, Q. L. & Chen, S. F. (2018), Botryosphaeriaceae from eucalyptus plantations and adjacent plants in China, *Persoonia: Molecular Phylogeny and Evolution of Fungi*, 40(June). https://doi.org/10.3767/persoonia.2018.40.03.
9. Li, Y., Pu, M., Cui, Y., Gu, J., Chen, X., Wang, L., Wu, H., Yang, Y. & Wang, C. (2023), Research on the isolation and identification of black spot disease of Rosa chinensis in Kunming, China, *Scientific Reports*, 13(1), 8299. https://doi.org/10.1038/s41598-023-35295-1.
10. Yildiz, A., Benlioglu, S., Benlioglu, K. & Korkom, Y. (2022), Occurrence of twig blight and branch dieback of walnut caused by Botryosphaeriaceae species in Turkey, *Journal of Plant Diseases and Protection*, 129(3), 687–693. https://doi.org/10.1007/s41348-022-00591-x.

11. Espinoza, J. G., Briceño, E. X., Chávez, E. R., Úrbez-Torres, J. R. & Latorre, B. A. (2009), Neofusicoccum spp. associated with stem canker and dieback of blueberry in Chile, *Plant Disease*, 93(11). https://doi.org/10.1094/PDIS-93-11-1187.

12. Glass, N. L. & Donaldson, G. C. (1995), Development of primer sets designed for use with the PCR to amplify conserved genes from filamentous ascomycetes, *Applied and Environmental Microbiology*, 61(4). https://doi.org/10.1128/aem.61.4.1323-1330.1995.

13. White, T. J., Bruns, T., Lee, S. & Taylor, J. (1990), Amplification and Direct Sequencing of Fungal Ribosomal Rna Genes for Phylogenetics: PCR - Protocols and Applications - A Laboratory Manual, In *PCR Protocols: A Guide to Methods and Applications* (Issue 1).

14. Hall, T. A. (1999), BIOEDIT: a user-friendly biological sequence alignment editor and analysis program for Windows 95/98/ NT, *Nucleic Acids Symposium Series*, 41.

15. Kumar, S., Stecher, G., Li, M., Knyaz, C. & Tamura, K. (2018), MEGA X: Molecular evolutionary genetics analysis across computing platforms, *Molecular Biology and Evolution*, 35(6). https://doi.org/10.1093/molbev/msy096.

16. Minh, B. Q., Schmidt, H. A., Chernomor, O., Schrempf, D., Woodhams, M. D., Von Haeseler, A., Lanfear, R. & Teeling, E. (2020), IQ-TREE 2: New Models and Efficient Methods for Phylogenetic Inference in the Genomic Era, *Molecular Biology and Evolution*, 37(5). https://doi.org/10.1093/molbev/msaa015.

17. Kalyaanamoorthy, S., Minh, B. Q., Wong, T. K. F., Von Haeseler, A. & Jermiin, L. S. (2017), ModelFinder: Fast model selection for accurate phylogenetic estimates, *Nature Methods*, 14(6). https://doi.org/10.1038/nmeth.4285.

18. Letunic, I. & Bork, P. (2021), Interactive tree of life (iTOL) v5: An online tool for phylogenetic tree display and annotation, *Nucleic Acids Research*, 49(W1). https://doi.org/10.1093/nar/gkab301.

19. Bezerra, J. D. P., Crous, P. W., Aiello, D., Gullino, M. L., Polizzi, G. & Guarnaccia, V. (2021), Genetic diversity and pathogenicity of botryosphaeriaceae species associated with symptomatic citrus plants in Europe, *Plants*, 10(3). https://doi.org/10.3390/plants10030492.

20. Hilário, S., Lopes, A., Santos, L. & Alves, A. (2020), Botryosphaeriaceae species associated with blueberry stem blight and dieback in the Centre Region of Portugal. *European Journal of Plant Pathology*, 156(1). https://doi.org/10.1007/s10658-019-01860-6.

21. Lopes, A., Barradas, C., Phillips, A. J. L. & Alves, A. (2016), Diversity and phylogeny of Neofusicoccum species occurring in forest and urban environments in Portugal, *Mycosphere*, 7(7). https://doi.org/10.5943/mycosphere/si/1b/10.

22. Iturritxa, E., Slippers, B., Mesanza, N. & Wingfield, M. J. (2011), First report of Neofusicoccum parvum causing canker and die-back of Eucalyptus in Spain, *Australasian Plant Disease Notes*, 6(1). https://doi.org/10.1007/s13314-011-0019-5.

23. Yildiz, A., Benlioglu, S., Benlioglu, K. & Korkom, Y. (2022). Occurrence of twig blight and branch dieback of walnut caused by Botryosphaeriaceae species in Turkey, *Journal of Plant Diseases and Protection*, 129(3). https://doi.org/10.1007/s41348-022-00591-x.

24. Berraf-Tebbal, A., Guereiro, M. A. & Philips, A. J. L. (2014), Phylogeny of Neofusicoccum species associated with grapevine trunk diseases in Algeria, with description of Neofusicoccum algeriense sp. nov., *Phytopathologia Mediterranea*, 53(3). https://doi.org/10.14601/Phytopathol_Mediterr-14385.

25. Alberti, I., Prodi, A., Nipoti, P. & Grassi, G. (2018), First report of Neofusicoccum parvum causing stem and branch canker on Cannabis sativa in Italy, *Journal of Plant Diseases and Protection*, 125(5). https://doi.org/10.1007/s41348-018-0174-4.

26. Roberts, A. J. & Punja, Z. K. (2022), Pathogenicity of seedborne Alternaria and Stemphylium species and stem-infecting Neofusicoccum and Lasiodiplodia species to cannabis (Cannabis sativa L., marijuana) plants, *Canadian Journal of Plant Pathology*, 44(2). https://doi.org/10.1080/07060661.2021.1988712.

27. Manca, D., Bregant, C., Maddau, L., Pinna, C., Montecchio, L. & Linaldeddu, B. T. (2020), First report of canker and dieback caused by Neofusicoccum parvum and Diplodia olivarum on oleaster in Italy, *Italian Journal of Mycology*, 49. https://doi.org/10.6092/issn.2531-7342/11048.

28. Zhixing, W., Yahong, Z., Yu, F., Qiyu, W., Jiani, L., Min, Y., Yu, Z., Lei, Y. & Feiyan, H. (2022), First report of Neofusicoccum parvum causing stem blight and dieback of Osmanthus fragrans in China, *Journal of Plant Pathology*, 104(1). https://doi.org/10.1007/s42161-021-00936-9.

29. Choi, S., Paul, N. C., Lee, K. H., Kim, H. J. & Sang, H. (2021), Morphology, molecular phylogeny, and pathogenicity of neofusicoccum parvum, associated with leaf spot disease of a new host, the Japanese bay tree (Machilus thunbergii), *Forests*, 12(4). https://doi.org/10.3390/f12040440.

30. Xu, D., Xi, P., Xu, J., Lin, Z., Jiang, Z. & Qiao, F. (2022), Association of Neofusicoccum parvum with leaf scorch on Cinnamomum cassia in China, *Forest Pathology*, 52(1). https://doi.org/10.1111/efp.12726.

31. Slippers, B., Boissin, E., Phillips, A. J. L., Groenewald, J. Z., Lombard, L., Wingfield, M. J., Postma, A., Burgess, T. & Crous, P. W. (2013), Phylogenetic lineages in the Botryosphaeriales: A systematic and evolutionary framework. *Studies in Mycology*, 76. https://doi.org/10.3114/sim0020.

MOLECULAR PHYLOGENY OF *LASIODIPLODIA THEOBROMAE* ASSOCIATED WITH *NELUMBO NUCIFERA* IN THUA THIEN HUE, VIETNAM AND THEIR SENSITIVITY TO SILVER NANOPARTICLES

Vu Quang Hoang Nguyen[1], Quang Tan Hoang[1], Lan Thuy Tran[1], Tram Tran Thi Ngoc[1], Hoang Thi Kim Hong[2*]

[1]*Institute of Biotechnology, Hue University, Thua Thien Hue, Vietnam*

[2]*Biotechnology Department, College of Medicine and Pharmacy, Duy Tan University, Da Nang, Vietnam*

SUMMARY

In Vietnam, lotus is a plant with cultural and spiritual significance, representing purity, spiritual growth, and enlightenment. *Lasiodiplodia* fungi are associated with a wide range variety of host worldwide along with endophytes, pathogens, and saprobes. In this study, symptomatic leaves of *Nelumbo nucifera* were collected from Thua Thien Hue Provinces and *Lasiodiplodia theobromae* are characterized, identified based on combined sequence data analyses (multi locus) of internal transcribed spacer (ITS), beta tubulin (*tub2*), and translation elongation factor 1-alpha (*tef-1α*) coupled with morphological characteristics. Furthermore, AgNPs showed potent activity against *L. theobromae* at a concentration of 30 μg mL^{-1}, a 73.72% inhibition of mycelial growth was observed for the pathogen *L. theobromae* VNHUCC.NEL38 at 3 days post-inoculation. Thus, the present study indicates AgNPs may have considerable antifungal activity, these findings will contribute to the development of effective management strategies to control these diseases and improve lotus production

Keywords: Lasiodiplodia theobromae, *Nelumbo nucifera*, phylogeny, Vietnam, silver nanoparticles.

INTRODUCTION

Lasiodiplodia genus (Botryosphaeriaceae family, Botryosphaeriales) was first described by Clendenin in 1896 and is represented by *L. tubericola*, which is now recognized as *L. theobromae* (Phillips *et al*., 2013; Dou *et al*., 2017). This genus with characterized by large, ovoid to oblong, usually hyaline, aseptate ascospores and hyaline or pigmented, aseptate, one or rarely multi-septate, conidia usually with longitudinal striations. Both sexual and asexual morphs have been recorded for *Lasiodiplodia* genus. The family Botryosphaeriaceae consists of a group (monophyletic lineage) of 22 genera that are distinguished based on their ascospores and conidia, as well as their phylogenetic relationships. Conidiophores are typically reduced to conidiogenous cells, which, when present, are characterized by hyaline, cylindrical conidiophores that are sometimes septate and rarely branched *Lasiodiplodia* species have subglobose or oval smooth, thick-walled conidia that are initially hyaline and become dark brown and striated when mature

Distinguishing between *Lasiodiplodia* species based on morphological features alone is challenging and unreliable, leading to inaccurate identification because of their similar cultural and conidial characteristics. Hence, a DNA sequencing approach is recommended for accurate species identification, as well as clear phylogenetic boundaries. Recent research has advanced the recognition of various *Lasiodiplodia* species using sequence data of multi-locus with the internal transcribed spacers (ITS), partial translation elongation factor-1α (t*ef1*), and partial β-tubulin (*tub2*) with high phylogenetic support. *Lasiodiplodia* species are wide distribution, commonly found in tropical and subtropical regions and exhibit different lifestyles as endophytes, pathogens, and saprobes. These species have been known to infect various crops, including almonds (*Prunus amygdalus*), blueberries (*Vaccinium corymbosum*), baobabs, citrus fruits (*Citrus* spp.), cocoa (*Theobroma cacao*), coconuts (*Cocos nucifera*), grapevines (*Vitis* spp.), durians (*Durio* spp.), dragon fruits (*Hylocereus polyrhizus*), groundnuts (*Arachis hypogaea*), jackfruits (*Artocarpus heterophyllus*), mango (*Mangifera indica*), mulberries (*Morus* spp.), olives (*Olea europaea*), pines (*Pinus* spp.), strawberries (*Fragaria* spp.), and rice (*Oryza* spp.) (Berraf-Tebbal *et al*. 2020; El-Ganainy *et al*. 2022; Ko *et al*. 2023). There are few studies on *Lasiodiplodia*-associated leaf disease in *Nelumbo nucifera*. Therefore, the current study aimed to characterize *Lasiodiplodia* isolates from *Nelumbo nucifera* in Thua Thien Hue Province, Vietnam, using morphological and phylogenetic analyses based on ITS, *tef-1α,* and *tub2* sequence data. In addition, assessing the sensitivity of fungal reactions to AgNPs will provide essential knowledge regarding their potential use as plant protection products. This information is crucial for sustainable breeding and the design of management strategies against fungicide-resistant strains.

MATERIALS AND METHODS

Sample Collection and Fungal Isolation

Symptomatic leaf samples were collected, and stored in plastic at Gene Laboratory, Institute of Biotechnology, Vietnam, where isolation was subsequently conducted. Fungal isolation was performed using the tissue

transplantation method. Pieces of symptom-containing healthy parts of 5 × 5 mm were cut and surface disinfected using 70% ethanol and 1% a.i sodium hypochlorite (NaOCl). Then, washed 3 times with sterile distilled water (DW), and dried on sterile filter paper. The samples were placed directly on water agar (WA) and incubated at ambient temperature (28 ± 2 °C) for 2-3 days. Hyphal tips recovered from the infected tissues were cut and directly placed on potato dextrose agar (PDA; HiMedia, India) for purification. The obtained fungal samples were transferred to PDA slant/PDA-glycerol and preserved at -40 °C for further analyses. To induce sporulation, isolates were transferred to 2 % water agar with sterilized pine needles on the agar surface (PNA).

DNA Extraction, PCR Amplification, and Sequencing

Each fungal isolate was cultured on PDA for 5 days to obtain young mycelia, which were subjected to DNA extraction using the Genomic DNA Extraction Kit following the manufacturer's instructions (ABT, Vietnam). Portions of internal-transcribed spacer (ITS), translation elongation factor 1-α (*tef1-α*), and β-tubulin (*tub2*) regions were amplified using the primer pairs ITS1/ITS4 (White *et al*., 1990), EF1-728F/ EF-986R (Carbone and Kohn, 1999), and Bt2a/Bt2b (Glass and Donaldson, 1995), respectively (Table 1). PCR amplification was performed in 60 uL reaction volume containing 30 µL of Go Taq Green 2x Master Mix (Promega, USA), 5 µL of the DNA template (50 ng), 5 µL of each primer (10 pmol), and 15 µL of ddH_2O. PCR profile was denatured at 95 °C for 3 min, followed by 35 cycles of 95 °C for 30 s, annealing at 52 °C (ITS), 55°C (*tef-1α,* and *tub2)* for 30 s, elongation at 72 °C for 1 min, and a final extension at 72 °C for 10 min. The PCR products were observed via 1% agarose electrophoresis gel using SafeView staining.

Table 1. Gene regions and respective primer pairs were used in the study.

Locus	Gene region	Primer	Sequence (5'-3')
internal transcribed spacer regions with intervening 5.8S nrRNA gene	ITS	ITS1	TCC GTA GGT GAA CCT GCGG
		ITS4	TCC TCC GCT TAT TGA TAT GC
Partial beta-tubulin gene	*tub2*	Bt2a	GGT AAC CAA ATC GGT GCT GCT TTC
		Bt2b	ACC CTC AGT GTA GTG ACC CTT GGC
Partial translation elongation factor 1-alpha	*tef*	EF1-728F	CAT CGA GAA GTT CGA GAA GG
		EF1-986R	TAC TTG AAG GAA CCC TTA CC

Phylogenetic analyses

A portion of the PCR product was sequenced by the sequencing service provider First BASE Laboratories (Seri Kembangan, Malaysia). A BLASTn search was used to compare the sequences found in our study with other sequences deposited for similarity analysis in those of Genebank - NCBI (National Center for Biotechnology Information, https://blast.ncbi.nlm.nih.gov/Blast.cgi, accessed on 15 December 2023) database. Sequences for each locus were constructed and aligned in MAFFT v7.487 using default settings and trimmed using trimAl 2.rev0 b g. Gaps were deemed to be missing data, and ambiguously aligned areas were discarded. The alignment was further manually adjusted using BioEdit v. 7.0.9.0 if necessary.To establish the identity of the isolates at species level, phylogenetic analyses were conducted individually for individual loci and then as combined analyses of three loci (ITS, TEF, and TUB2) based on maximum likelihood (ML) in IQ-TREE. The ModelFinder was used to determine the best-fit model (Kalyaanamoorthy *et al*., 2017). Branch support was determined using 10,000 ulfabootstraps, a Bayesian posterior probabilities support and 10,000 SH-aLRT bootstrap replicates. The resulting trees were plotted using FigTree v. 1.4.2 (http://tree.bio.ed.ac.uk/software/figtree), and Interactive Tree of Life (iTOL) v.5 (Letunic and Bork, 2021), and further edited using PowerPoint (Microsoft, CA, USA) and Adobe Illustrator CC 2021 (Adobe Systems, San Jose, CA, USA).

Pathogenicity assay

Young and healthy leaves of *Nelumbo nucifera* were collected, washed with tap water, and surface-disinfected with 1% sodium hypochlorite. They were then submerged in 70% ethanol for 1 min and rinsed twice with sterilized water. One piercing wound was made in the mid-region of each leaf using a sterilized needle to form a tiny dot. Mycelium plugs (6 × 6 mm) of ½ PDA were cut from an actively growing colony, placed at the inoculation points, and wrapped in parafilm. The plants were kept under high humidity conditions (>85% relative humidity) in a covered plastic container for 1–3 days at 28 °C. Sterile PDA plugs were used to inoculate the control plants. The non-wounding experiment was conducted similarly without causing any damage to the leaves. The petri dishes were placed inside a plastic box, and the leaves were incubated at 25 °C with humidity and a 12/12-hour fluorescent light/dark cycle. After five days, the leaves were examined for symptom development, and the diameter of the diseased spot was measured.

Antifungal effects of AgNPs against *L. theobromae*

An *in vitro* assay was carried out on PDA with 0.1, 1, 10, 20, and 30 mg/L of silver nanoparticles (AgNPs). Stock nanoparticle solution was transferred into PDA to obtain different initial AgNPs concentrations (0.1, 1, 10, 20 and

30 mgL^{-1}). Medium containing AgNPs was poured into 90 × 15 mm petri dishes and incubated at room temperature. After 48 h of incubation, an agar plug of 6x6 mm diameter containing fungi was inoculated simultaneously at the center of each Petri dish and incubated at 28 ± 2°C. Culture medium without AgNPs was inoculated and cultured under the same conditions as the control treatment. The size of the colonies was measured after 1, 2,3, 7 days and each treatment was replicated. The mycelial growth inhibition rate – MGIR (%) was calculated using the following formula: where R is the radial growth of fungi in the control plate, and r is the radial growth of fungi in silver nanoparticle treated plates.

$$MGRI(\%) = \frac{R_{control} - R_{treated}}{R_{control}}$$

RESULTS & DICCUSSION

Symptom Recognition and Fungal Isolates

The disease appeared as small irregular brown spots on the lotus leaves (only recorded as aerial/standing leaves), originating from the outer leaf margins or damaged leaf areas. Subsequently, the spots enlarged and coalesced into regular or irregular brown necrotic lesions with dark-brown margins. Lesions on leaf petioles were characterized by brown areas, separating the color between infected and non-diseased areas. On PDA, the fungal isolates produced dense fast-growing mycelia. Colonies with abundant aerial mycelia reached the lid, covering the surface of the Petri plate after 3-4 days. Initially, the aerial mycelium was white to pale gray or smoke-gray colonies, gradually becoming dark grayish on the surface and reversing with age. (Fig. 1E). The conidia were immature and mature. Both immature and mature conidia were ovoid to ellipsoid in shape and 1-septate, with longitudinal striations, a broadly rounded apex, and tapering to the truncated base. Based on the morphological characteristics of the fungal isolates, we identified the recorded isolates as *Lasiodiplodia* sp., which was consistent with the morphology described by Alves và đồng tác giả (2008).

Five strains of *Lasiodiplodia* isolated from leaves (aerial leaf) and petioles of *Nelumbo nucifera* in Thua Thien Hue Province, Vietnam, were grown in culture. From the five isolates, two representative isolates were selected for molecular analysis based on a combined analysis of ITS, *TUB2*, and *TEF* gene sequences. The final dataset comprised of 79 taxa of representative isolates of *Lasidodiplodia* genus, including two isolates obtain in this study. *Diplodia multila* (CMW7060) is used as the outgroup taxon. Phylogenetic analysis revealed that the topologies of the ML trees generated from individual and concatenated genes (ITS, *tef1-α*, and *tub2*) were similar.

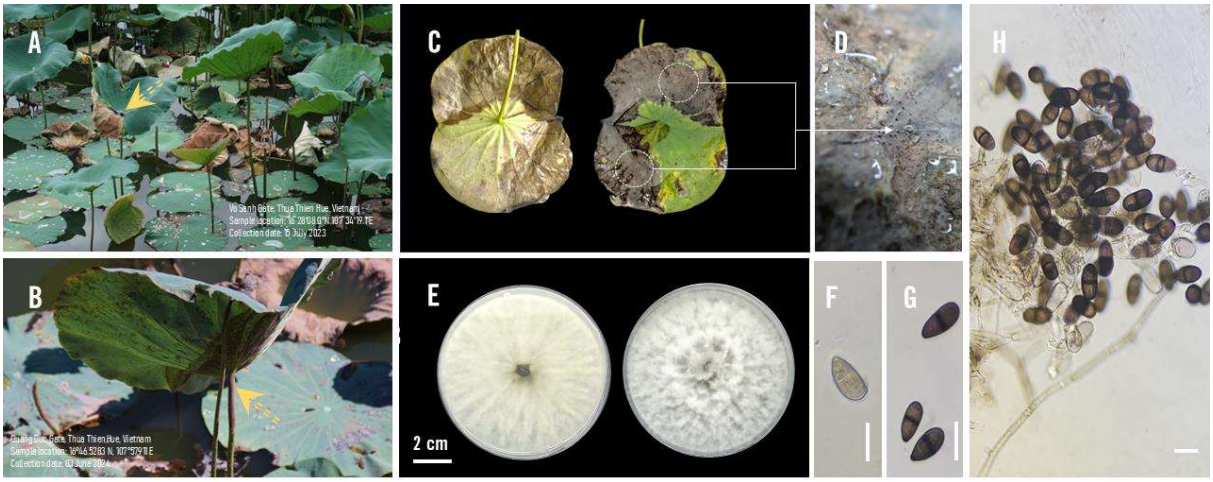

Figure 1. A, B. Symptomatic leaf samples observed in the lotus (N. nucifera) field. C, D. Zoomed in view of lesions with black pycnidia; E. Top and bottom view of VNHUCC.NEL38 colony on PDA; F: immature conidia; G: mature conidia with longitudinal striations; H: Conidia and fungal mycelia. Scale: E: 2cm; F-G: 15µm; H: 10µm.

The dataset combined alignment included 80 sequences (taxa) with 1261 characters, including gaps. ML analysis indicated 355 distinct patterns, 165 parsimony-informative, 98 singleton sites, 998 constant sites. The ML tree was contrusted with optimal log-likelihood value of -4925.922. Estimated base frequencies were as follows: A: 0.207, C: 0.306, G: 0.257, T: 0.231, rate parameters: A-C: 1.00000; A-G: 4.03082; A-T: 1.00000; C-G: 1.00000; C-T: 4.03082; G-T: 1.00000. Proportion of invariable sites: 0.614. Gamma distribution shape alpha: 0.776. Best-fit model: HKY+F+I+G4 chosen according to Bayesian Information Criterion (BIC), TIM3+F+I+G4 according Akaike Information Criterion (AIC). Two isolates VNHUCC.NEL38, VNHUCC.NEL107 developed a cluster with *L. theobromae*, (Fig. 2). Notably, within the same cluster, our two isolates developed distinct evolutionary lengths with these *L. theobromae* isolates CBS 164.96 (TYPE strain), CBS 11530, IBL375 (Pitomba - *Talisia esculenta*,

Brazil), MFLUCC 17-0379 (stem of *Hevea brasiliensis,* Thailand). The combined ITS, tef1 and tub2 phylogeny showed that *Lasiodiplodia theobromae* (including VNHUCC.NEL38, VNHUCC.NEL107) clades sister to *L. laosensis, L. brasiliense*, and *Lasiodiplodia bruguierae* with high support (85.9/1/91). As a result, all the present two isolates (VNHUCC.NEL38, VNHUCC.NEL107) were verified as *L. theobromae* by virtue of molecular identification and phylogenetic analysis.

Genus *Lasiodiplodia* is cosmopolitan and most species can be found primarily in tropics and subtropics. Many phytopathogenic fungal species with widespread distribution can be found within this genus, responsible for causing over 500 plant diseases such as fruit rot, root rot, collar rot, stem-end rot, dieback, canker, and leaf necrosis. In Vietnam, *Lasiodiplodia* species have been associated with various destructive diseases, such as fruit rot of jackfruit (*Artocarpus heterophyllus)* in DakLak*,* stem end rot disease in pomelo (*Citrus maxima*) and mango in Ben Tre; gummosis on Thanh Tra pomelo *Citrus grandis* in Thua Thien Hue (Khuong *et al*., 2023; Thao *et al*., 2023; Trai *et al*., 2024). Recently, Cuong và đồng tác giả (2023) also reported *L. theobromae* as the causative agent of blight disease in lotus plants (Cuong *et al*., 2023). Notably, all these reports indicated that *L. theobromae* is the causative agent of the disease. To date, there have been no instances of any other species within the *Lasiodiplodia* genus.

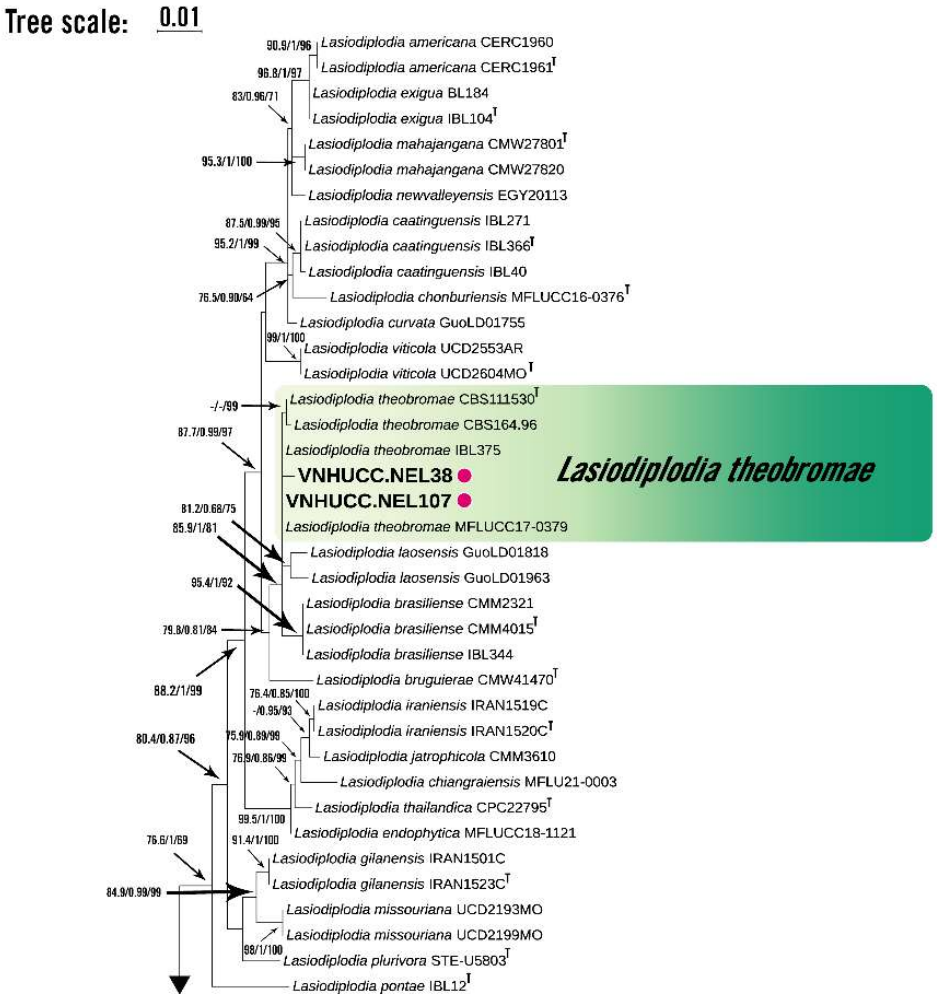

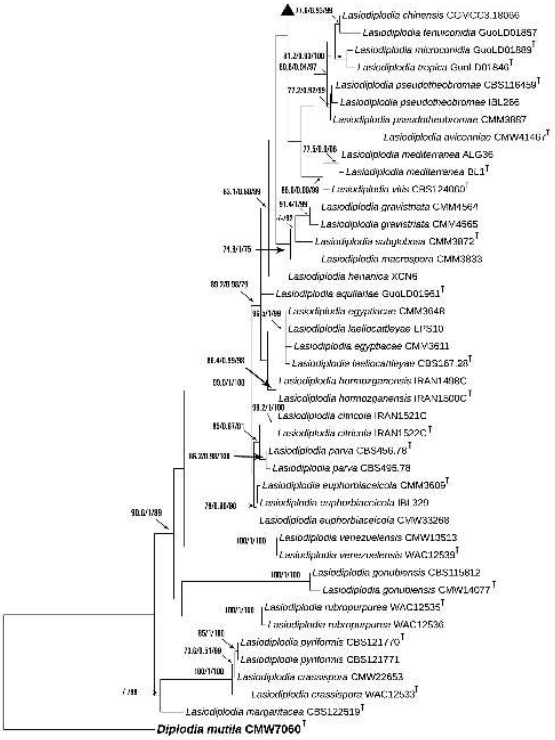

Figure 2. Maximum likelihood (ML) tree of the *Lasiodiolodia* species. *Diplodia mutila* CMW7060 was selected as the outgroup. At the nodes, bootstrap support values for ML (≥ 70%) and BYPP (≥ 0.5), SH-aLRT (≥ 75%) are displayed (SH-aLRT /BYPP/ML). Ex-type isolates are marked with "T", and our isolates obtained from this study are in bold. The scale bar indicates 0.01 nucleotide changes per site

Pathogenicity test

All isolates of *Lasiodiplodia* were pathogenic to detached leaves of lotus, resulting in visible lesions 5 days after inoculation. The symptoms observed both on the surface and internally were dark brown necrotic lesions that extended upward and downward from the point of inoculation on both wounded and unwounded samples. Lesion development in wounded samples was found to be more rapid and severe than in unwounded samples. No visible symptoms were observed in control leaves. The lotus cultivars differed significantly in the severity of foliar symptoms caused by *L. theobromae*. Two lotus varieties in Hue showed that *L. thebromae* only causes disease in the Cao san lotus variety, while the white lotus variety has no symptoms. Notably, when tested using the isolated wound method, the leaves had larger diameter lesions (114 mm), leading to visible lesions five days after infection, whereas in the non-wounded method, the lesions progressed very slowly, were barely visible, or were small (24.34 mm). Symptoms observed both on the surface and internally were dark brown necrotic lesions extending up and down (light brown) from the inoculation site in both the wounded and non-wounded methods.

Antifungal effects of AgNPs against *L. theobromae*

To determine the sensitivity of *L. theobromae* (VNHUCC.NEL38) to silver nanoparticles (AgNPs), different concentrations of were used to generate fungitoxicity curves and determine the concentration of AgNPs needed to inhibit colony growth by 50% (EC50 values). Mycelial plugs of the VNHUCC.NEL38 isolates were inoculated on PDA plates containing various concentrations of AgNPs (0, 0.1, 1, 10, 20, and 30 µg mL^{-1}) and PC (broad spectrum fungicide - hexaconazole 500 µg mL^{-1})

The effectiveness of the silver nanomaterials in inhibiting the growth of *L. theobromae* VNHUCC.NEL38 was assessed. One day after inoculation (1dpi), all concentrations exhibited a certain level of inhibition compared wih the control. However, after 2 dpi, the rapid mycelial growth of *Lasiodiplodia* species resulted in no significant differences between the control and low concentration (0.1 - 1 µg mL^{-1}) PDA plates. At higher concentrations (10 µg mL^{-1} and 20 µg mL^{-1}), the inhibition rate was 13.76%-16.27%. The concentration of 30 mg/L resulted in a high level of inhibition (73.72%). This level of inhibition was maintained at 30 µg mL^{-1} after 72 h (72.39%), whereas the remaining concentrations were no longer different from that of the control. Additionally, an inhibitory effect of up to 54.51%.was observed at a concentration of 30 µg mL^{-1} even 7 days after inoculation. VNHUCC.NEL38 also exhibited high sensitivity to PC-hexaconazole (500 µg mL^{-1}), with a relatively high inhibition rate ranging from 46.31% to 57.33% on the first and second day after inoculation. However, the inhibitory efficacy of hexaconazole against *L. theobromae* decreased rapidly by the third day of exposure, reaching 15.37%.

In conclusion, the inhibitory efficacy of AgNPs is highly dependent on the concentration and duration of exposure. In our experiment, at low concentrations (0.1 – 1 µg mL^{-1}), AgNPs have very little inhibitory effect. At high concentrations (30 mL^{-1}), AgNPs exhibit strong inhibition of mycelial growth, but this effect may decrease over time. This suggests that the effectiveness of silver compounds also depends on the duration of their expose. Tarazona (2019) demonstrated complete inhibition of the mycelium growth of *F. graminearum, F. culmorum, F. sporotrichioides, F. langsethiae, F. poae, F. proliferatum* and *F. verticillioides* after the longest exposure (20–30 h) to citrate-stabilized AgNP at concentarions of 30 and 45 mg L^{-1} (Tarazona *et al*., 2019). The antifungal activity of AgNPs is attributed to their ability to modify fungal colony morphology and disrupt cell membranes. In a study, Linh và đồng tác giả (2021) identified pathogen-caused stem-end rot mango fruits in Vietnam as *L. theobromae* XB1. In addition, nano-Cu at 4000 ppm inhibited fungal *L. theobromae* XB1 growth by 52.4% after seven days. Silver nanoparticles had a limited effect, with the highest inhibition of 80% at 400 ppm, and no growth at 25 ppm. Previous studies have reported that silver nanoparticles damage the transport system, leading to an outflow of intracellular ions and disruption of cellular processes such as metabolism and respiration. Previous studies by Xia và đồng tác giả have indicated that *Trichosporon asahii* organelles, including mitochondria, chromatin, and ribosomes, sustained significant damage when exposed to AgNPs (Xia *et al*., 2016)

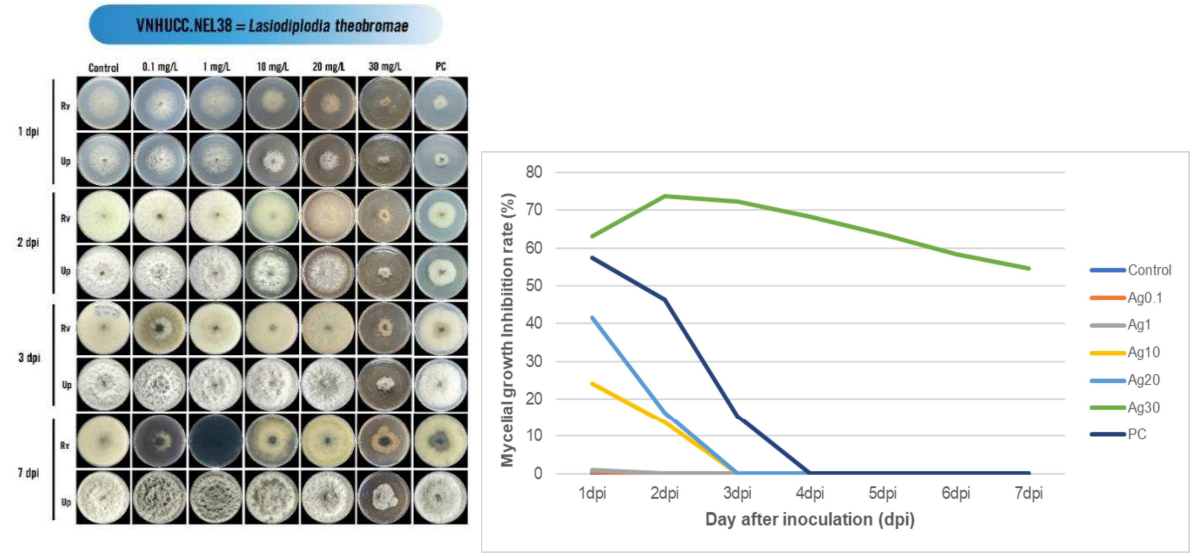

Figure 3. Mycelial growth inhibition (MGIR, %) of *L. theobromae* VNHUCC.NEL38 after application of AgNPs at different concentrations

CONCLUSION

In the current study, pathogens causing leaf blight, dieback petioles of *Nelumbo nucifera* in Thua Thien Hue, Vietnam were identified as *L. theobromae* based on morphological and molecular studies of multiple DNA sequences. This study has expanded the knowledge for disease management of *L. theobromae* in vitro by using silver nanoparticles.

Acknowledgments: *This work was supported by grant of Hue University (Grant number code: DHH2023-15-20).*

Nguyen Quang Hoang Vu was funded by Vingroup Joint Stock Company and supported by the Domestic Ph.D. Scholarship Programme of Vingroup Innovation Foundation (VINIF), Vingroup Big Data Institute (VINBIGDATA), code: [VINIF.TS.2020.TS.89; VINIF.2021.TS.145; VINIF.2022.TS.147].

REFERENCES

Alves A, Crous PW, Correia A, Phillips AJL. (2008). Morphological and molecular data reveal cryptic speciation in Lasiodiplodia theobromae. *Fungal Divers*. 28.

Berraf-Tebbal A, Mahamedi AE, Aigoun-Mouhous W, Špetík M, Čechová J, Pokluda R, Baránek M, Eichmeier A, Alves A. (2020). Lasiodiplodia mitidjana sp. nov. And other Botryosphaeriaceae species causing branch canker and dieback of Citrus sinensis in Algeria. *PLoS One*. 15(5). https://doi.org/10.1371/journal.pone.0232448

Dou ZP, He W, Zhang Y. (2017). Does morphology matter in taxonomy of Lasiodiplodia? An answer from Lasiodiplodia hyalina sp. nov. *Mycosphere*. 8(2). https://doi.org/10.5943/mycosphere/8/2/5

El-Ganainy SM, Ismail AM, Iqbal Z, Elshewy ES, Alhudaib KA, Almaghasla MI, Magistà D. (2022). Diversity among Lasiodiplodia Species Causing Dieback, Root Rot and Leaf Spot on Fruit Trees in Egypt, and a Description of Lasiodiplodia newvalleyensis sp. nov. *Journal of Fungi*. 8(11). https://doi.org/10.3390/jof8111203

Kalyaanamoorthy S, Minh BQ, Wong TKF, Von Haeseler A, Jermiin LS. (2017). ModelFinder: Fast model selection for accurate phylogenetic estimates. *Nature Methods*. 14(6). https://doi.org/10.1038/nmeth.4285

Khuong NQ, Nhien DB, Thu LTM, Trong ND, Hiep PC, Thuan VM, Quang LT, Thuc LV, Xuan DT. (2023). Using *Trichoderma asperellum* to Antagonize Lasiodiplodia theobromae Causing Stem-End Rot Disease on Pomelo (Citrus maxima). *Journal of Fungi*. 9(10). https://doi.org/10.3390/jof9100981

Ko YZ, Liyanage WK, Shih HC, Tseng MN, Shiao MS, Chiang YC. (2023). Unveiling Cryptic Species Diversity and Genetic Variation of Lasiodiplodia (Botryosphaeriaceae, Botryosphaeriales) Infecting Fruit Crops in Taiwan. *Journal of Fungi*. 9(9). https://doi.org/10.3390/jof9090950

Letunic I, Bork P. (2021). Interactive tree of life (iTOL) v5: An online tool for phylogenetic tree display and annotation. *Nucleic Acids Research*. 49(W1). https://doi.org/10.1093/nar/gkab301

Phillips AJL, Alves A, Abdollahzadeh J, Slippers B, Wingfield MJ, Groenewald JZ, Crous PW. (2013). The Botryosphaeriaceae: Genera and species known from culture. *Studies in Mycology*. 76:51–167. https://doi.org/10.3114/sim0021

Tarazona A, Gómez J V., Mateo EM, Jiménez M, Mateo F. (2019). Antifungal effect of engineered silver nanoparticles on phytopathogenic and toxigenic Fusarium spp. and their impact on mycotoxin accumulation. *International Journal of Food Microbiology*. 306. https://doi.org/10.1016/j.ijfoodmicro.2019.108259

Thao LD, Hien LT, Trang TTT, Trinh PT, Tuan DK. (2023). First report of *Lasiodiplodia theobromae* causing fruit rot of jackfruit in Vietnam. *Indian Phytopatholy*. 76(4). https://doi.org/10.1007/s42360-023-00684-z

Trai VTN, Ha TTT, Hung NB. (2024). First Report of *Lasiodiplodia theobromae* Causing Gummosis on Citrus grandis (L.) Osbeck in Vietnam. *Research in Plant Disease*. 30(1):78–81. https://doi.org/10.5423/RPD.2024.30.1.78

Cuong HV, Ha TTT, Thao LQ, Thúy HTT, Vinh LV. (2023). Xác định nguyên nhân gây bệnh tàn lụi cây sen tại Thừa Thiên Huế năm 2022. *Vietnam Journal of Agricultural Sciences.* 21(5): 529-542

Xia ZK, Ma QH, Li SY, Zhang DQ, Cong L, Tian YL, Yang RY. (2016). The antifungal effect of silver nanoparticles on Trichosporon asahii. *Journal of Microbiology*, *Immunology and Infection*. 49(2). https://doi.org/10.1016/j.jmii.2014.04.013

PHÂN TÍCH PHÁT SINH LOÀI *LASIODIPLODIA THEOBROMAE* TRÊN CÂY SEN Ở THỪA THIÊN HUẾ VÀ ĐÁNH GIÁ MỨC ĐỘ NHẠY CẢM VỚI VẬT LIỆU NANO BẠC

Nguyễn Quang Hoàng Vũ[1*], Hoàng Tấn Quảng[1], Trần Thúy Lan[1], Trần Thị Ngọc Trâm[1], Hoàng Thị Kim Hồng[2*]

[1]*Viện Công nghệ sinh học, Đại học Huế, Thừa Thiên Huế, Việt Nam*

[2]*Khoa Công nghệ sinh học, Trường Y Dược, Đại học Duy Tân, Đà Nẵng, Việt Nam*

TÓM TẮT

Ở Việt Nam, sen là loài cây có ý nghĩa văn hóa tâm linh, tượng trưng cho sự thanh khiết, nghị lực trường tồn, đóng vai trò quan trọng vững chắc trong văn hóa tâm linh và tôn giáo. Nấm *Lasiodiplodia* đã được biết với hệ thống vật chủ đa dạng trên thế giới cùng với nhiều dạng sống từ: nội sinh, mầm bệnh gây hại và hoại sinh. Trong nghiên cứu này, các lá có triệu chứng điển hình của cây sen (*Nelumbo nucifera*) được thu thập từ các điểm trồng sen tại tỉnh Thừa Thiên Huế và phân lập. Kết quả *Lasiodiplodia theobromae* được xác định dựa trên các đặc điểm hình thái đối chiếu với phân tích dữ liệu trình tự đa locus kết hợp của 3 vùng gene ITS, beta tubulin (*tub2*) và nhân tố giãn dài dịch mã 1α (*tef-1α*). Bên cạnh đó, thử nghiệm *in vitro* với các hạt nano bạc cho thấy tiềm năng kháng nấm mạnh chống lại *L. theobromae*. Ở nồng độ 30 µg mL^{-1}, ghi nhận thấy mức độ ức chế lên đến 73,72% (3 ngày sau cấy) sự phát triển của sợi nấm đối với tác nhân gây bệnh phân lập được *L. theobromae* VNHUCC.NEL38 so với đối chứng. Do đó, nghiên cứu hiện tại chỉ ra rằng AgNP có thể có hoạt tính kháng nấm đáng kể, cần được nghiên cứu sâu hơn về quản lý bệnh sinh học, chương trình kiểm dịch. Những phát hiện này sẽ góp phần phát triển các chiến lược quản lý hiệu quả để kiểm soát các bệnh này và cải thiện quá trình canh tác, nâng cao năng suất cây sen trên địa bàn tỉnh Thừa Thiên Huế.

Từ khóa: *Lasiodiplodia theobromae*, *Nelumbo nucifera*, phân tích phát sinh loài, Việt Nam, nano bạc.

[*] Author for correspondence: Tel: +84-978939467; Email: hoangtkimhong@duytan.edu.vn

Journal of Phytopathology

WILEY

Journal of Phytopathology

SHORT COMMUNICATION

First Report of *Colletotrichum plurivorum* Causing Anthracnose on the Aquatic Plant (*Nelumbo nucifera*) From Vietnam

Vu Quang Hoang Nguyen[1] | Thi Thi Diem Pham[1] | Lan Thuy Tran[1] | Tram Thi Ngoc Tran[1] | Hoang Tan Quang[1] | Hoang Thi Kim Hong[2,3]

[1]Institute of Biotechnology, Hue University, Hue, Vietnam | [2]Biotechnology Department, College of Medicine and Pharmacy, Duy Tan University, Da Nang, Vietnam | [3]Institute for Global Health Innovations, Duy Tan University, Da Nang, Vietnam

Correspondence: Hoang Thi Kim Hong (hoangtkimhong@duytan.edu.vn)

Received: 13 July 2025 | **Revised:** 13 August 2025 | **Accepted:** 19 September 2025

Funding: This work was supported by Hue University (Grant code: DHH2023-15-20). Vu Quang Hoang Nguyen was funded by Vingroup Joint Stock Company and supported by the Domestic Ph.D. Scholarship Programme of Vingroup Innovation Foundation (VINIF), Vingroup Big Data Institute (VINBIGDATA), code: [VINIF.2020.TS.89; VINIF.2021.TS.145; VINIF.2022.TS.147].

Keywords: anthracnose | *Colletotrichum plurivorum* | *Nelumbo nucifera* | phylogenetic analyses | plant pathogens

ABSTRACT

Nelumbo nucifera, commonly known as the sacred lotus, holds significant cultural, medicinal, nutritional and ecological importance in Vietnam. Despite its importance, the cultivation of this aquatic plant is frequently threatened by a variety of pathogens, which pose serious challenges to crop health and productivity. During the 2023–2024 growing season, typical symptoms of anthracnose were observed on white lotus plants (*Nelumbo nucifera* cv. white). The disease initially appears as concentric circular spots with irregular dark brown patterns that typically develop in the central area of the leaves. These lesions progressively expand toward the leaf margins, eventually coalescing to form larger necrotic lesions. Morphological identification, phylogeny of five loci: ITS, *GAPDH, ACT, CHS1* and *TUB2* genes, and a pathogenicity test of the fungus from symptomatic inoculated plants confirmed *Colletotrichum plurivorum* as the causative agent of the disease. To our knowledge, this is the first report of *Colletotrichum plurivorum* causing anthracnose in white lotus (*Nelumbo nucifera*) in Vietnam.

1 | Introduction

Lotus (*Nelumbo nucifera*) is a beautiful and pure flower, symbolically associated with Buddhism, as well as cultural and historical significance (Li et al. 2014). Additionally, the lotus plant holds considerable economic value linked to the diversity of local specialty products and ecological landscape factors. All parts of the lotus plant—including the flower, leaves, lotus rhizomes and seeds—are utilised in culinary dishes and as medicinal ingredients with valuable applications in traditional medicine (Pokhrel et al. 2022; Sharma et al. 2017).

In the 2023 and 2024 cultivation seasons, lotus ponds planted with the Hue white lotus variety recorded the occurrence of anthracnose disease on leaves. The typical symptoms included irregular, concentric, brown to dark brown necrotic spots on the adaxial leaf surface, whereas the same lesions appeared light brown on the abaxial side. This disease was observed on approximately 30% of the total lotus cultivation area in ponds at Phu Xuan Ward, Hue, Vietnam. The presence of anthracnose poses a significant threat to the health and productivity of the lotus crops, necessitating timely monitoring and effective disease management strategies to minimise yield losses.

Anthracnose, caused by fungi belonging to the genus *Colletotrichum*, represents a major threat to crop health and yield worldwide. Species within this genus are not only well-known plant pathogens but also function as saprobes and endophytes, colonising a broad spectrum of plant hosts. Due to their widespread impact and diversity, *Colletotrichum* species are considered among the top 10 most important groups of plant pathogens globally (Dean et al. 2012). Therefore, precise identification of *Colletotrichum* species is essential for implementing effective disease management strategies and preventing further spread of infection. However, species delimitation within this genus is often complicated by overlapping morphological characteristics and variable host associations. Traditionally, the classification of *Colletotrichum* species has relied primarily on the morphological features of conidia and appressoria, supplemented by specific cultural characteristics observed under controlled growth conditions. Nevertheless, many species exhibit highly similar morphological traits that are frequently influenced by environmental factors such as culture medium, incubation period, light conditions, and temperature (Cai et al. 2009; Hyde et al. 2009; Jayawardena et al. 2021). Given the extensive species diversity—1078 *Colletotrichum* names currently recorded in Index Fungorum (accessed April 05, 2025)—reliance solely on morphological features or single-locus molecular markers such as the internal transcribed spacer (ITS) region is insufficient for accurate species resolution. Premature taxonomic conclusions based on limited methodologies have resulted in widespread misidentifications and inaccurate annotations of *Colletotrichum* species in public databases such as GenBank. Moreover, these shortcomings have contributed to the complexity and inconsistency in the delineation of species within this genus.

This situation underscores the urgent need for a robust and precise taxonomic framework for the genus *Colletotrichum*, which encompasses some of the most economically significant phytopathogens worldwide, including those affecting valuable crops in Vietnam. Accordingly, this study aimed to identify the causal agents of anthracnose on *Nelumbo nucifera* in Hue, Vietnam, by combining a taxonomic classification system, detailed morphological characterisation, and multi-locus phylogenetic analyses.

2 | Materials and Methods

Leaf tissue pieces measuring approximately 0.5×0.5 cm were excised from the margin between healthy and diseased areas. These tissue samples were surface-sterilised by consecutively immersing them in 75% ethanol for 30 s, 1% sodium hypochlorite (NaClO) for 30 s, and then rinsing three times with sterile water. The tissue pieces were dried on sterilised filter paper and placed onto potato dextrose agar (PDA, Himedia). All PDA plates were incubated in the dark at 28°C for 1–2 days. Hyphal tips resembling *Colletotrichum* colonies were transferred to fresh PDA medium for further cultivation. Colonies were purified at least twice until pure cultures were obtained.

Fungal genomic DNA was extracted directly from 7-day-old pure cultures using the Genomic DNA Extraction Kit (ABT, Vietnam) following the manufacturer's instructions. The gene sequences of the following genomic regions were amplified: rDNA internal transcribed spacer (ITS), actin (*ACT*), chitin synthase 1 (*CHS*1), β-tubulin (*TUB*2) and glyceraldehyde-3-phosphate dehydrogenase (*GAPDH*). The primers used for amplification are listed in Table 1.

Each PCR reaction mixture had a total volume of 60 μL, consisting of 5 μL each of forward and reverse primers (10 μM), 30 μL of 2× PCR Master Mix, 12.5 μL of deionised water (ddH_2O), and 5 μL of DNA template. The PCR program consisted of an initial denaturation at 95°C for 5 min, followed by 32 cycles of denaturation at 95°C for 50 s, annealing at 55°C for 50 s for ITS, 50°C for 1 min for *GAPDH* and *ACT*, and 58.5°C for 1 min for *CHS*1, *TUB*2, and *ACT*, with an extension step at 72°C for 1 min and a final extension at 72°C for 7 min. PCR amplicons were purified and sequenced at the FirstBase Laboratories Sdn Bhd (Malaysia). The sequences obtained were deposited in the GenBank nucleotide database.

Phylogenetic analysis utilised DNA sequence data retrieved from the GenBank database (http://www.ncbi.nlm.nih.gov/genbank/, Table 2). Multiple sequences were aligned using the MAFFT v.7.110 (http://mafft.cbrc.jp/alignment/server/) and adjusted manually in MEGA v.7.2 (Kumar et al. 2018). To establish the species-level identity of the isolates, phylogenetic analysis was conducted using a combined dataset of five single-locus

TABLE 1 | Primer used in this study.

Gene/locus	Primer	Sequence (5′–3′)	References
Internal transcribed spacer (ITS)	ITS1	GGA AGT AAA AGT CGT AAC AAG G	White et al. (1990)
	ITS4	TCC TCC GCT TAT TGA TAT GC	
Glyceraldehyde-3-phosphate dehydrogenase (*GAPDH*)	GDF1	GCC GTC AAC GAC CCC TTC ATT GA	Guerber et al. (2003)
	GDR1	GGG TGG AGT CGT ACT TGA GCA TGT	
Actin (*ACT*)	ACT-512F	ATGTGCAAGGCCGGTTTCGC	Carbone and Kohn (1999)
	ACT-783R	TAC GAG TCC TTC TGG CCC AT	
β-tubulin (*TUB*2)	Bt2a	GGTAACCAAATCGGTGCTGCTTTC	Glass and Donaldson (1995)
	Bt2b	ACCCTCAGTGTAGTGACCCTTGGC	
Chitin synthase 1 (*CHS*1)	CHS-79F	TGG GGC AAG GAT GCT TGG AAG AAG	Carbone and Kohn (1999)
	CHS-354R	TGG AAG AAC CAT CTG TGA GAG TTG	

TABLE 2 | Taxa with their respective GenBank accession numbers used in the phylogenetic analyses.

Species	Isolates	Host	Country	Genbank accession numbers				
				ITS	*GAPDH*	*CHS-1*	*ACT*	*TUB2*
Colletotrichum cattleyicola	**CBS 170.49**[a]	*Cattleya* sp.	Belgium	MG600758	MG600819	MG600866	MG600963	MG601025
C. cliviicola	**CBS 125375**[a]	*Clivia miniata*	China	MG600733	MG600795	MG600850	MG600939	MG601000
C. monsterae	**LC13871 = NN055214**[a]	*Monstera deliciosa*	China	MZ595897	MZ664121	MZ799351	MZ664195	MZ674015
C. musicola	**CBS 132885**[a]	*Musa* sp.	Mexico	MG600736	MG600798	MG600853	MG600942	MG601003
C. orchidearum	**CBS 135131**[a]	*Dendrobium nobile*	Netherlands	MG600738	MG600800	MG600855	MG600944	MG601005
C. pereskiae	**VIC 47381**[a] **= COAD 2995**	*Pereskia aculeata*	Brazil	MZ262421	MZ265337	N/A	N/A	N/A
C. piperis	**IMI 71397 = CPC 21195**[a]	*Piper nigrum*	Malaysia	MG600760	MG600820	MG600867	MG600964	MG601027
C. plurivorum	**CBS 125474**[a]	*Coffea* sp.	Vietnam	MG600718	MG600781	MG600841	MG600925	MG600985
	LC8240 = M51	*Paederia foetida*	China	MZ595848	MZ664113	MZ799291	MZ664146	MZ673969
	ZHKUCC 23–0867	*Impatiens balsamina*	China	OR286376	OR493878	OR493850	OR493822	OR453364
	GUCC 12141	*Piper sarmentosum*	China	OP723084	OP784117	OP730669	OP740205	OP761983
C. sojae	**ATCC 62257**[a]	*Glycine max*	USA	MG600749	MG600810	MG600860	MG600954	MG601016
C. syngoniicola	**LC8894 = M745**[a]	*Syngonium* sp.	China	MZ595863	MZ664117	MZ799296	MZ664161	MZ673982
C. vittalense	**CBS 181.82**[a]	*Theobroma cacao*	India	MG600734	MG600796	MG600851	MG600940	MG601001
	GUCC 12144	*Piper sarmentosum*	China	OP723092	OP784120	OP730672	OP740208	OP761986
C. reniforme	**LC8230**[a]	*Smilax cocculoides*	China	MZ595847	MZ664110	MZ799290	MZ664145	MZ673968
C. magnum **(OUTGROUP)**	**CBS519.97**[a]	*Citrullus lanatus*	USA	MG600769	MG600829	MG600875	MG600973	MG601036
C. merremiae **(OUTGROUP)**	**CBS 124955**[a]	*Merremia umbellata*	Panama	MG600765	MG600825	MG600872	MG600969	MG601032

Note: Bold font indicates the TYPE species strains. Strains used as OUTGROUP in the phylogenetic analysis are highlighted with a green box.
Abbreviation: N/A, not available.
[a]Ex-type or authentic culture.

alignments (ITS, *ACT, CHS-1, GAPDH* and *TUB2*) based on maximum likelihood (ML) in IQ-TREE (Minh et al. 2020). The ModelFinder was used to determine the best-fit model (Kalyaanamoorthy et al. 2017). Branch support was determined using 10,000 ulfabootstraps, a Bayesian posterior probabilities support, and 10,000 SH-aLRT bootstrap replicates. The resulting trees were plotted using Interactive Tree of Life (iTOL) v.5 (Letunic and Bork 2021), and further edited using PowerPoint (Microsoft, CA, USA) and Adobe Illustrator CC 2021 (Adobe Systems, San Jose, CA, USA).

3 | Results and Discussion

On PDA medium, after 7 days of cultivation, the colony diameter of *C. plurivorum* (VNHUCC.NEL92, VNHUCC.NEL102) averaged between 78.8 and 80.6 mm. Initially, the colony exhibited an off-white colour with a light, fluffy texture and even margins, while the reverse of the colony showed concentric rings, with the central rings having a darker pigmentation that gradually lightened toward the outer rings (Figure 1C). After 20 days, the colony colour shifted to off-white to light grey; simultaneously, fruiting body structures appeared as black spots scattered on the colony surface (Figure 1D–F). The sexual morph was observed on PDA. Under the microscope, the ascomata structures appeared light brown to dark brown, with the peridium composed of small, tightly arranged cells. The asci were two-layered, ranging from clavate to slightly curved cylindrical shapes, with smooth walls, containing 6–8 spores, and possessing a visible apical apparatus; they were translucent. The ascospores were translucent with smooth walls, ring-shaped to semicircular, slightly pointed at both ends (Figure 1K–O).

Two isolates (VNHUCC.NEL92 and VNHUCC.NEL102) belonging to the *Colletotrichum orchidearum* species complex were identified to species level based on phylogenetic analyses of five different loci (ITS, *GAPDH, CHS-1, ACT* and *TUB2*). Multi-locus data contained 1922 characters including gaps, 330 distinct patterns, 155 parsimony-informative sites, 137 singleton sites and 1630 constant sites. The best-scoring IQ-TREE, with a final optimization likelihood value of −4898.145, is presented. Estimated base frequencies were as follows: A = 0.221, C = 0.307, G = 0.256, T = 0.217; while the substitution rates parameters: A-C = 1.00000, A-G = 4.02349, A-T = 1.00000, C-G = 1.00000, CT = 6.47927, GT = 1.000000. The gamma distribution shape parameter $\alpha = 0.143$.

According to the phylogenetic tree, the results showed that both our isolates (VNHUCC.NEL92, VNHUCC.NEL102) clustered with different reference isolates of *C. plurivorum*, including the Ex-type strain CBS125474 (originally isolated from coffee plants in Vietnam), with strong support values at the nodes: SH-aLRT/BPP/MLBS of 92.5/1/94 at the node connecting the isolate to CBS125474, and 87.4/0.99/94 at the basal node of the clade containing all reference isolates of *C. plurivorum* used in this study. These reference isolates include LC8240 (*Paederia foetida*), GUCC12141 (*Piper sarmentosum*), and ZHKUCC 23-0867 (*Impatiens balsamina*), all reported from China. In the

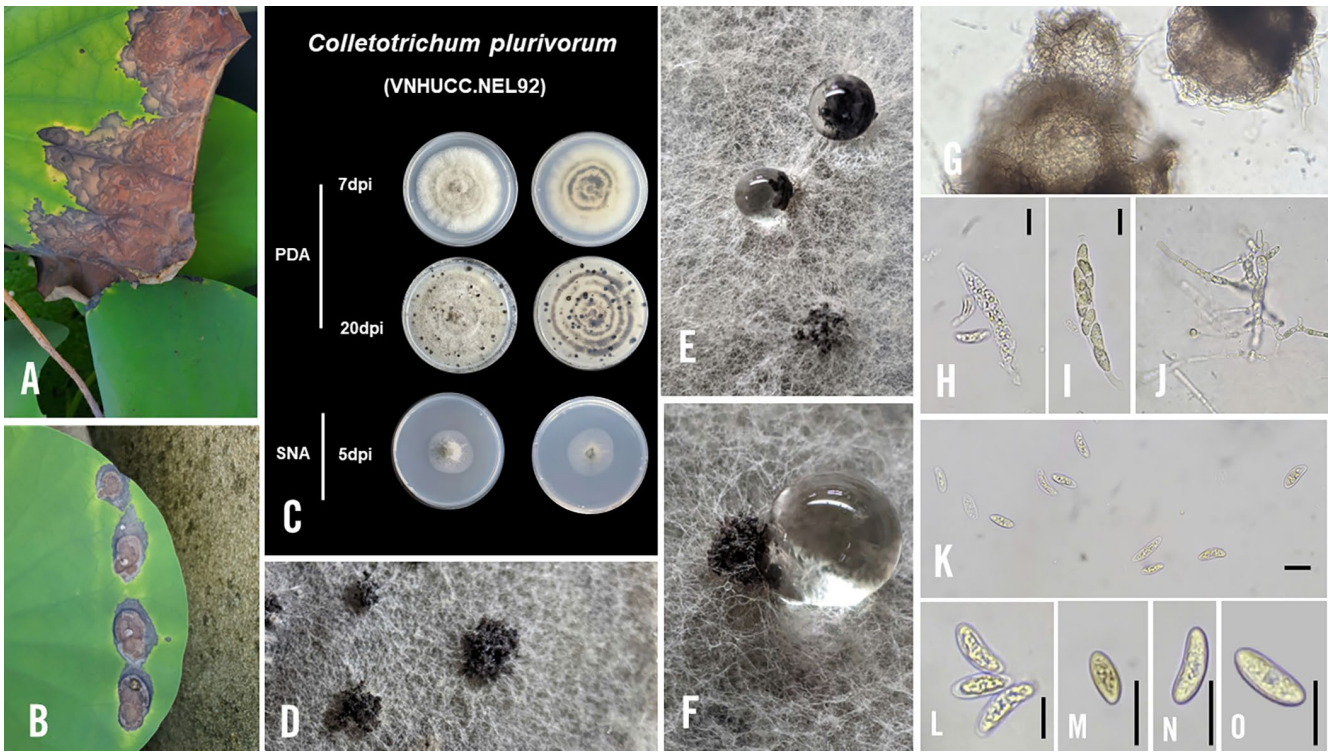

FIGURE 1 | Symptoms and morphological characteristics of *C. plurivorum* (VNHUCC.NEL92). (A) Symptoms of concentric brown rot recorded on white lotus plants; (B) Lesions resulting from artificial inoculation (non-wound inoculation); (C) Morphological features of the colony on PDA medium (at 7 and 20 days post-inoculation—dpi) and SNA medium (5 dpi); (D–F) Colony texture and morphology of ascomata on PDA medium; (G) Cross-section of the fruiting body structure and outer peridium layer (Ascoma & ascoma peridium); (H) Immature asci; (I) Mature asci; (J) Conidiophores; (K–O) Ascospores. Scale bar: 10 μm.

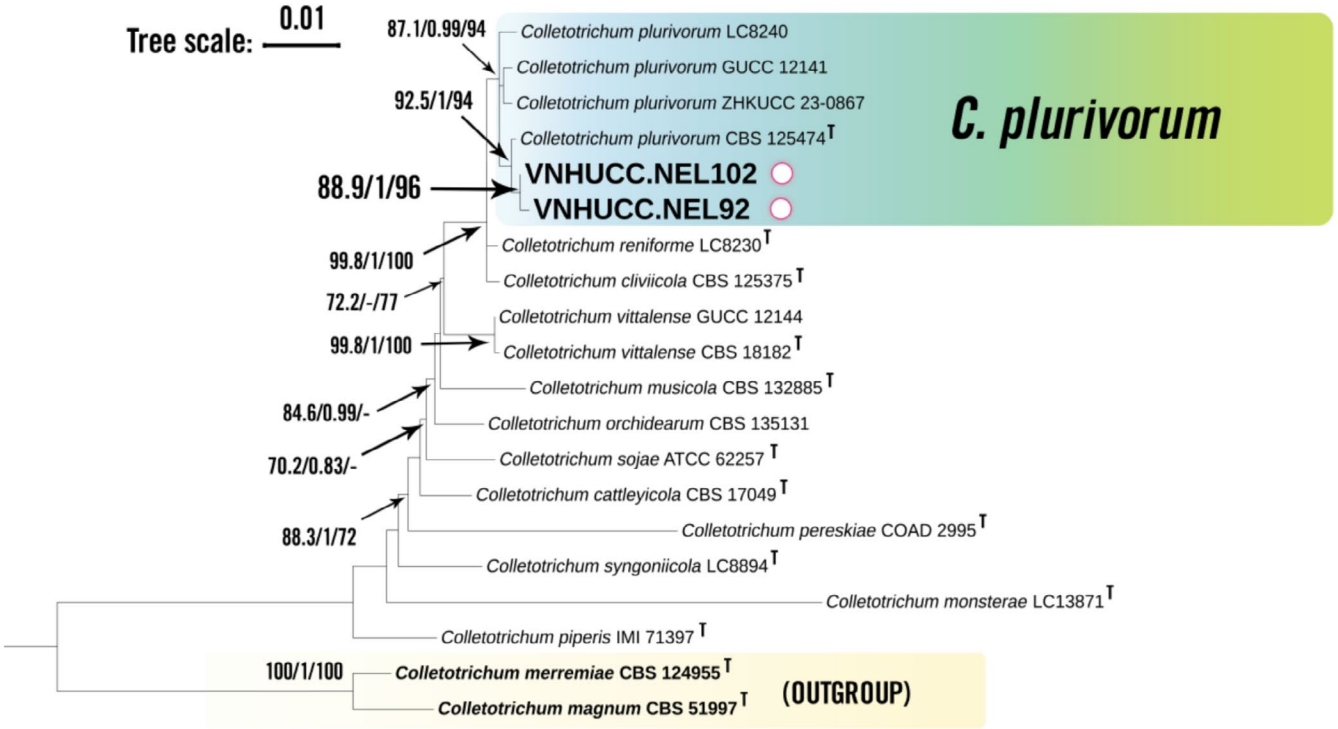

FIGURE 2 | Maximum likelihood (ML) phylogenetic tree of the *Colleotrichum orchidearum* species complex, including two representative isolates, VNHUCC.NEL92 and VNHUCC.NEL102 was constructed from a concatenated alignment dataset of five loci: ITS, *GAPDH, CHS-1, ACT* and *TUB2*. Support values of SH-aLRT > 70%/aBayes > 0.75/ML bootstrap (%) > 70% are shown at each node as SH-aLRT/BPP/MLBS. Two reference isolates, *C. merremiae* and *C. magnum*, were used as outgroups. The scale bar indicates the estimated number of substitutions per nucleotide site. The colour of the circles following each taxon corresponds to isolates obtained from white lotus cultivar (*N. nucifera*).

molecular phylogeny, *C. plurivorum* was closely related to *C. reniforme* (LC8230) and *C. cliviicola* (CBS 125375).

Furthermore, based on observed morphological features, the two isolates VNHUCC.NEL92 and VNHUCC.NEL102 closely resembled the original descriptions of *C. plurivorum* (Damm et al. 2019). By integrating multilocus (ITS, *GAPDH, ACT, CHS-1, TUB2*) phylogenetic evidence with morphological characters, both isolates are identified as *C. plurivorum* (Figure 2).

Historically, *Colletotrichum plurivorum* was first described as *C. sichuanensis* from fruits of *Capsicum annuum* in China (F. Liu et al. 2016). Subsequently, it was later considered a synonym of *C. cliviicola* by Douanla-Meli et al. (2018). However, Damm et al. (2019) distinguished *C. plurivorum* as a separate species based on comprehensive morphological and molecular data, clearly differentiating it from *C. cliviicola* (Damm et al. 2019).

Regarding its geographic distribution and host history, *C. plurivorum* has been primarily reported in tropical countries, spanning at least 13 countries and territories, with the majority concentrated in three regions: East Asia, South Asia, and Southeast Asia (11 out of 13) (Bragard et al. 2021; Dai et al. 2024; García-Estrada et al. 2020; Kurera et al. 2023; Liu et al. 2023).

To our knowledge, this is the first report of *Colletotrichum plurivorum* causing anthracnose in white lotus (*Nelumbo nucifera*) in Vietnam. This finding not only expands the host range but also the geographic distribution of this species. Accurate identification of the causal agent is crucial for effective disease management and preventing cross-infection to other economically important crops.

Author Contributions

Conceptualisation: Vu Quang Hoang Nguyen, Hoang Thi Kim Hong. Collection and morphological examinations: Vu Quang Hoang Nguyen, Tram Thi Ngoc Tran, Thuy Lan Tran. Molecular sequencing and phylogenetic analyses: Vu Quang Hoang Nguyen, Thi Thi Diem Pham, Hoang Tan Quang. Original draft preparation: Vu Quang Hoang Nguyen. Review and editing, supervision: Hoang Thi Kim Hong, Hoang Tan Quang, Vu Quang Hoang Nguyen. All authors have read and agreed to the published version of the manuscript.

Acknowledgements

This work was supported by Hue University (Grant code: DHH2023-15-20). Vu Quang Hoang Nguyen was funded by Vingroup Joint Stock Company and supported by the Domestic Ph.D. Scholarship Programme of Vingroup Innovation Foundation (VINIF), Vingroup Big Data Institute (VINBIGDATA), code: [VINIF.2020.TS.89; VINIF.2021.TS.145; VINIF.2022.TS.147].

Ethics Statement

The authors have nothing to report.

Conflicts of Interest

The authors declare no conflicts of interest.

Data Availability Statement

The sequencing data obtained in this study have been deposited in GenBank with accession numbers ITS (PV759434, PV759435), *CHS1* (PV929974, PV929975), *ACT* (PX000056, PX000057), *TUB2* (PX000058, PX000059), *GAPDH* (PX000060, PX000061).

References

Bragard, C., F. Di Serio, P. Gonthier, et al. 2021. "Pest Categorisation of *Colletotrichum plurivorum*." *EFSA Journal* 19, no. 11: 6886. https://doi.org/10.2903/j.efsa.2021.6886.

Cai, L., K. D. Hyde, P. Taylor, et al. 2009. "A Polyphasic Approach for Studying *Colletotrichum*." *Fungal Diversity* 39: 183–204.

Carbone, I., and L. M. Kohn. 1999. "A Method for Designing Primer Sets for Speciation Studies in Filamentous Ascomycetes." *Mycologia* 91, no. 3: 553–556. https://doi.org/10.2307/3761358.

Dai, Y., L. Gan, X. Liu, C. Lan, Z. Li, and X. Yang. 2024. "Occurrence of Leaf Spot Caused by *Colletotrichum plurivorum* on Cowpea in Fujian Province, China." *Crop Protection* 176: 106496. https://doi.org/10.1016/j.cropro.2023.106496.

Damm, U., T. Sato, A. Alizadeh, J. Z. Groenewald, and P. W. Crous. 2019. "The *Colletotrichum dracaenophilum, C. magnum* and *C. orchidearum* Species Complexes." *Studies in Mycology* 92: 1–46. https://doi.org/10.1016/j.simyco.2018.04.001.

Dean, R., J. A. L. Van Kan, Z. A. Pretorius, et al. 2012. "The Top 10 Fungal Pathogens in Molecular Plant Pathology." *Molecular Plant Pathology* 13: 414–430. https://doi.org/10.1111/j.1364-3703.2011.00783.x.

Douanla-Meli, C., J. G. Unger, and E. Langer. 2018. "Multi-Approach Analysis of the Diversity in *Colletotrichum cliviae* Sensu Lato." *Antonie Van Leeuwenhoek* 111, no. 3: 423–435. https://doi.org/10.1007/s10482-017-0965-9.

García-Estrada, R. S., I. Cruz-Lachica, L. A. Osuna-García, and I. Márquez-Zequera. 2020. "First Report of Papaya (*Carica papaya*) Anthracnose Caused by *Colletotrichum plurivorum* in Mexico." *Plant Disease* 104: 589. https://doi.org/10.1094/PDIS-05-19-0914-PDN.

Glass, N. L., and G. C. Donaldson. 1995. "Development of Primer Sets Designed for Use With the PCR to Amplify Conserved Genes From Filamentous Ascomycetes." *Applied and Environmental Microbiology* 61, no. 4: 1323–1330. https://doi.org/10.1128/aem.61.4.1323-1330.1995.

Guerber, J. C., B. Liu, J. C. Correll, and P. R. Johnston. 2003. "Characterization of Diversity in *Colletotrichum acutatum sensu lato* by Sequence Analysis of Two Gene Introns, mtDNA and Intron RFLPs, and Mating Compatibility." *Mycologia* 95, no. 5: 872–895. https://doi.org/10.1080/15572536.2004.11833047.

Hyde, K. D., L. Cai, E. H. C. McKenzie, Y. L. Yang, J. Z. Zhang, and H. Prihastuti. 2009. "Colletotrichum: A Catalogue of Confusion." *Fungal Diversity* 39: 1–17.

Jayawardena, R. S., C. S. Bhunjun, K. D. Hyde, E. Gentekaki, and P. Itthayakorn. 2021. "*Colletotrichum*: Lifestyles, Biology, Morpho-Species, Species Complexes and Accepted Species." *Mycosphere* 12, no. 1: 7. https://doi.org/10.5943/mycosphere/12/1/7.

Kalyaanamoorthy, S., B. Q. Minh, T. K. F. Wong, A. Von Haeseler, and L. S. Jermiin. 2017. "ModelFinder: Fast Model Selection for Accurate Phylogenetic Estimates." *Nature Methods* 14, no. 6: 587–589. https://doi.org/10.1038/nmeth.4285.

Kumar, S., G. Stecher, M. Li, C. Knyaz, and K. Tamura. 2018. "MEGA X: Molecular Evolutionary Genetics Analysis Across Computing Platforms." *Molecular Biology and Evolution* 35, no. 6: 1547–1549. https://doi.org/10.1093/molbev/msy096.

Kurera, W. M. S., N. K. B. Adikaram, D. M. D. Yakandawala, S. S. Maharachchikumbura, L. Jayasinghe, and K. Samarakoon. 2023. "Molecular and Phenotypic Characterization of *Colletotrichum plurivorum* and *Colletotrichum musae* Causing Banana Anthracnose Disease in the Central Province of Sri Lanka." *Journal of the National Science Foundation of Sri Lanka* 51, no. 2: 11217. https://doi.org/10.4038/jnsfsr.v51i2.11217.

Letunic, I., and P. Bork. 2021. "Interactive Tree of Life (iTOL) v5: An Online Tool for Phylogenetic Tree Display and Annotation." *Nucleic Acids Research* 49, no. W1: W293–W296. https://doi.org/10.1093/nar/gkab301.

Li, Y., P. Svetlana, J. Yao, and C. Li. 2014. "A Review on the Taxonomic, Evolutionary and Phytogeographic Studies of the Lotus Plant (Nelumbonaceae: Nelumbo)." *Acta Geologica Sinica* 88, no. 4: 1252–1261. https://doi.org/10.1111/1755-6724.12287.

Liu, F., G. Tang, X. Zheng, et al. 2016. "Molecular and Phenotypic Characterization of *Colletotrichum* Species Associated With Anthracnose Disease in Peppers From Sichuan Province, China." *Scientific Reports* 6: 32761. https://doi.org/10.1038/srep32761.

Liu, Y., Y. Shi, D. Zhuo, et al. 2023. "Characterization of Colletotrichum Causing Anthracnose on Rubber Trees in Yunnan: Two New Records and Two New Species From China." *Plant Disease* 107, no. 10: 3037–3050. https://doi.org/10.1094/PDIS-11-22-2685-RE.

Minh, B. Q., H. A. Schmidt, O. Chernomor, et al. 2020. "IQ-TREE 2: New Models and Efficient Methods for Phylogenetic Inference in the Genomic Era." *Molecular Biology and Evolution* 37, no. 5: 1530–1534. https://doi.org/10.1093/molbev/msaa015.

Pokhrel, T., D. Shrestha, K. Dhakal, P. M. Yadav, and A. Adhikari. 2022. "Comparative Analysis of the Antioxidant and Antidiabetic Potential of *Nelumbo nucifera* Gaertn. And *Nymphaea lotus* L. Var. *pubescens* (Willd.)." *Journal of Chemistry* 2022: 1–5. https://doi.org/10.1155/2022/4258124.

Sharma, B. R., L. N. S. Gautam, D. Adhikari, and R. Karki. 2017. "A Comprehensive Review on Chemical Profiling of *Nelumbo Nucifera*: Potential for Drug Development." *Phytotherapy Research* 31: 3–26. https://doi.org/10.1002/ptr.5732.

White, T. J., T. Bruns, and J. Taylor. 1990. "Amplification and Direct Sequencing of Fungal Ribosomal RNA Genes for Phylogenetics." In *A Guide to Molecular Methods and Applications*, edited by M. A. Innis, D. H. Gelfand, J. J. Sninsky, and J. W. White, 315–322. Academic Press. https://doi.org/10.1016/B978-0-12-372180-8.50042-1.